Soil Parameterization in Land Surface Models Drives Large Discrepancies in Soil Moisture Predictions Across Hydrologically Complex regions Regions of the Contiguous United States

Kachinga Silwimba¹, Alejandro N. Flores¹, Irene Cionni¹, Sharon A. Billings², Pamela L. Sullivan³, Hoori Ajami⁴, Daniel R. Hirmas⁵, and Li Li⁶

Correspondence: Kachinga Silwimba (kachingasilwimba@u.boisestate.edu)

Abstract. Land surface models (LSMs) are critical components of Earth system models (ESMs), enabling simulations of energy and water fluxes essential for understanding climate systems. Soil hydraulic parameters, derived using pedotransfer functions (PTFs), are key to modeling soil-plant-water interactions but introduce uncertainties in soil moisture predictions. However, a key knowledge gap exists in understanding how specific soil hydraulic properties contribute to these uncertainties and in identifying the regions most affected by them. This study assesses the influence of soil parameter settings on soil moisture variability in the Community Land Model version 5 (CLM5) over the contiguous United States (CONUS) using Empirical Orthogonal Function (EOF) analysis. EOF analysis identified dominant spatial and temporal soil moisture patterns across multiple experimental configurations and highlighted the impact of soil parameter variability on hydrological processes. The results revealed significant discrepancies in soil moisture simulations, particularly in the central Great Plains, potentially due to the combination of arid climate conditions and limitations in modeling saturated hydraulic conductivity and soil water retention curves. Seasonal soil moisture dynamics aligned broadly with observed patterns but showed biases in magnitude and phase, emphasizing the need for refined parameterization, such as improving the representation of infiltration and drainage processes. Comparisons with ERA5-Land reanalysis data revealed improved alignment in regions with consistent climatic gradients but persistent model deficiencies in hydrologically complex areas, particularly under more arid climates such as the Great Plains, where hydrological processes are notoriously harder to reproduce. The This research highlights the necessity of refining soil parameter representations, utilizing high-resolution datasets, and considering climatic variability to boost the performance of LSMs. Importantly, these findings also open the door to future efforts that incorporate dynamic soil properties into LSMs. Much of this work demonstrates the dynamism of soil properties, and while this study advances modeling by revealing the importance of their inclusion, the next crucial step will be developing approaches that allow these properties to

¹Department of Geosciences, Boise State University, Boise, ID, USA

²Department of Ecology and Evolutionary Biology and Kansas Biological Survey & Center for Ecological Research, University of Kansas, Lawrence, KS, USA

³College of Earth, Ocean, and Atmospheric Science, Oregon State University, Corvallis, OR, USA

⁴Department of Environmental Sciences, University of California Riverside, Riverside, CA, USA

⁵Department of Plant and Soil Science, Texas Tech University, Lubbock, TX, USA

⁶Department of Civil and Environmental Engineering, Pennsylvania State University, University Park, PA, USA

be dynamic within LSMs. This paper serves as a foundational step toward that goal, paving the way for more complex and integrated modeling frameworks that better capture soil-hydrology-climate interactions.

1 Introduction

35

Land surface models (LSMs) are essential components of Earth system models (ESMs), offering critical insights into the movement and partitioning of energy and water across the Earth's surface, which are fundamental processes in understanding and simulating climate systems accurately (Kang and Hong, 2008; Zhao et al., 2017; Guimberteau et al., 2017; Hagemann et al., 2013; Dagon et al., 2020). Designed to operate on large spatial scales, LSMs rely on robust parameterizations of land processes, including the use of pedotransfer functions (PTFs) to parameterize soil hydraulic properties. PTFs, as described by Van Looy et al. (2017) and De Lannoy et al. (2014), are mathematical formulations that use extensive soil hydraulic databases to establish empirical relationships between soil particle-size distribution and soil hydraulic parameters, such as field capacity, permanent wilting point, saturated hydraulic conductivity, pore-size distribution, and soil water retention curves (McNeill et al., 2018; Vereecken et al., 2010; Weber et al., 2020). These PTFs range in complexity from basic linear models to advanced machine learning algorithms such as artificial neural networks (da Silva et al., 2023; Schaap et al., 1998). These soil hydraulic parameters are fundamental to quantification of soil moisture and water flow, and soil-plant-water interactions and their effects on climate, agriculture, hydrology, and environmental engineering.

PTFs play a crucial role in converting readily available soil texture data into soil hydraulic parameters, addressing the difficulties of acquiring accurate soil moisture data at larger scales (Fu et al., 2023). However, many soil hydraulic parameters are derived from laboratory or small-scale field studies, which often fail to capture the full heterogeneity of larger areas, limiting their representativeness (Lai and Ren, 2016; Godoy et al., 2018). To overcome this limitation, global soil texture maps enhance PTFs' predictive capabilities, enabling their application in regions where field measurements are unavailable and making them indispensable for land modeling (Tafasca et al., 2020; Dai et al., 2019). Soil moisture, a key output of these models, is a vital variable governing the exchange of water and energy between land and atmosphere. It has profound impacts on climate systems, vegetation dynamics, and extreme events, including droughts and floods (Zhang et al., 2021).

The influence of soil hydraulic properties on soil moisture simulations is well documented. For example, Fu et al. (2023) demonstrated that these properties significantly affect soil moisture simulations at the ELBARA field site in the northeast of the Tibetan Plateau, using the one-dimensional (1D) Richards equation. Similarly, Fu et al. (2022) noted that the numerical solution approach of the Community Land Model (Lawrence et al., 2019) produces a narrow range of soil hydraulic property values, which suggests a relatively weak influence on soil moisture simulations within this range. However, when optimized hydraulic properties are used, potentially derived to capture site-specific variability or improve model performance beyond this narrow range they can exert a more substantial influence on soil moisture dynamics. Furthermore, Feki et al. (2018) highlighted that saturated hydraulic conductivity exhibits the highest sensitivity to temporal changes in environmental factors, such as precipitation or temperature variability significantly affecting soil moisture variability, as shown in FEST-WB model simulation of a maize field in the Secugnago region. These findings underscore the importance of accurately representing soil

hydraulic properties, which directly influence the partitioning of water into runoff, infiltration, and evapotranspiration (Ye et al., 2023), as well as the temporal and spatial variability of soil moisture. However, uncertainties in parameterizations, such as the soil water retention curve that links water potential to volumetric soil moisture, continue to challenge the predictive capacity of LSMs, especially under extreme climatic conditions (Koster et al., 2004; De Lannoy et al., 2014). Improving the representation of soil moisture and its underlying hydraulic properties is critical, as it affects global hydrological cycles, vegetation health, and energy flows, all of which are essential for understanding and mitigating the impacts of climate change events (Oleson et al., 2010).

60

75

In addition to these complexities, scaling point-scale or regional observations of soil moisture to the coarser resolutions of LSM outputs presents a persistent challenge. While observational networks and remote sensing missions have expanded the availability of soil moisture data, the heterogeneous nature of soil properties combined with varying retrieval algorithms and coverage gaps can introduce significant uncertainties, both in terms of the accuracy of satellite products and their limitations for validating LSM outputs (Famiglietti, 2014; Brocca et al., 2017). Moreover, uncertainties in parameterization make it challenging to accurately simulate soil moisture dynamics, as noted by Reichle et al. (2004) and Kato et al. (2007), limiting the ability of LSMs to replicate observed soil moisture datasets. This discrepancy in spatial resolution and data precision can make model calibration more challenging, increase uncertainties in estimating parameters, and, as a result, weaken confidence in simulation outputs. Emerging evidence further complicates this issue by highlighting that soil properties can change over relatively short time scales due to shifts in climate and land cover. The dynamic nature of soil properties introduces additional pressure to better understand soil-hydraulic relationships and integrate these temporal dynamics into land surface models LSMs, as demonstrated by studies highlighting how climate and land cover changes influence soil processes (Hirmas et al., 2018; Koop et al., 2023; Caplan et al., 2019; Sullivan et al., 2022; Hauser et al., 2022). Addressing these complexities demands robust, data-oriented approaches and dimensionality reduction techniques to disentangle the effects of parameterization on soil moisture patterns across ecosystems and climate conditions.

A major challenge to addressing these uncertainties is the high dimensionality of LSM simulations when applied to continental or global scales, making it difficult to isolate the effects of specific parameters on soil moisture from other factors such as meteorological forcings and modes of climate variability Ji et al. (2023); Li et al. (2013); Zeng et al. (2021)(Ji et al., 2023; Li et al., 2013; Zeng et al. (2013)(Ji et al., 2023; Li et al., 2013; Zeng et al. (2013)(Ji et al., 2023; Li et al., 2013; Zeng et al. (2013)(Ji et al., 2023; Li et al., 2013; Zeng et al. (2013)(Ji et al., 2023; Li et al., 2013; Zeng et al. (2013)(Ji et al., 2023; Li et al., 2023; Li et al., 2013; Zeng et al. (2013)(Ji et al., 2023; Li

the advancement of land surface modeling and the comprehension of climate dynamics. Finally, they conclude with practical recommendations for upcoming research and applications in the fields of ecohydrology and climate science.

2 Data and Methods

90 2.1 Study Region

100

105

110

115

The study area depicted in Figure 1 covers region for this analysis encompasses the CONUS, which extends spanning from the Atlantic to the Pacific Ocean and is bordered bounded by Canada to the north and Mexico to the south. This region features a diverse range of climate zones, including (Figure 1). This domain covers a wide range of latitudes, elevations, and climatic regimes, offering an ideal natural laboratory for evaluating spatial variability in land surface processes. The CONUS includes major climate zones such as humid continental, Mediterranean, subtropical, arid, and alpine, all shaped by its extensive geographic reach and varied topography. Such climatic variance plays a crucial role in influencing soil moisture patterns, leading to dynamic variations throughout CONUS. The region's topographical elements, like of which emerge due to differences in latitude, topographic relief, and proximity to moisture sources such as the Gulf of Mexico and Pacific Ocean. These climatic gradients play a critical role in controlling soil moisture dynamics by modulating processes such as infiltration, evaporation, and water retention. Topographic features, including the Rocky Mountains, Appalachian Mountains, Sierra Nevada, and Cascade Range, significantly affect precipitation patterns, runoff, and soil characteristics, further contributing to soil moisture variability. Additionally, land cover types vary significantly, with moisture-rich forested areas and urban regions with limited infiltration capacity introducing further complexity to and Appalachian Mountains, significantly influence precipitation regimes and surface hydrology. These orographic barriers modify storm tracks and induce spatial variability in rainfall and snowpack accumulation, ultimately affecting soil water availability. The land cover across the CONUS is equally heterogeneous, ranging from forested regions in the Northeast and Pacific Northwest to urbanized corridors and sparsely vegetated deserts in the Southwest. This heterogeneity in land cover introduces additional complexity into soil moisture behavior, as vegetation, impervious surfaces, and soil types interact to determine local infiltration and storage dynamics.

To support spatially disaggregated analysis of soil moisture distribution. To improve the analysis of climate, topography, and land cover interactions on soil moisture dynamics, this study employs the regional subdivisions of CONUS suggested by Giorgi and Francisco (2000). As illustrated in Figure 1, the area is divided into four primary climate zonesvariability and its driving mechanisms, we adopt the regional classification scheme proposed by Giorgi and Francisco (2000), which partitions CONUS into four climatically and geographically coherent macro-regions: Western North America (WNA), Central North America (CNA), Eastern North America (ENA), and North Central America (NCA). These subdivisions enable a more detailed examination of soil moisture variability within distinct climatic and geographic contexts, providing valuable insights into the processes affecting soil moisture dynamics. This classification provides a physically grounded framework for evaluating the sensitivity of modeled soil moisture to soil hydraulic parameterizations across distinct hydroclimatic zones. As shown in Figure 1, each region captures dominant physiographic and climatic attributes, such as the arid basins and mountain ranges of WNA.

the agricultural plains and grasslands of CNA, the humid subtropical and deciduous forest zones of ENA, and the transitional climatic conditions present in NCA. The utility of this framework is two-fold. First, it facilitates regional intercomparison of soil moisture patterns and their controls, enabling consistent evaluation across diverse landscapes. Second, it improves the interpretability of EOF modes by linking observed spatial variability to regional climatic drivers, soil texture distributions, and vegetation structure. This regionalized approach is particularly valuable given the goal of disentangling parameter driven soil moisture responses from broader meteorological forcings. By leveraging the CONUS domain and its subdivisions, the study advances understanding of how soil hydraulic parameter uncertainty manifests across large-scale gradients and informs the development of improved land surface model parameterizations.

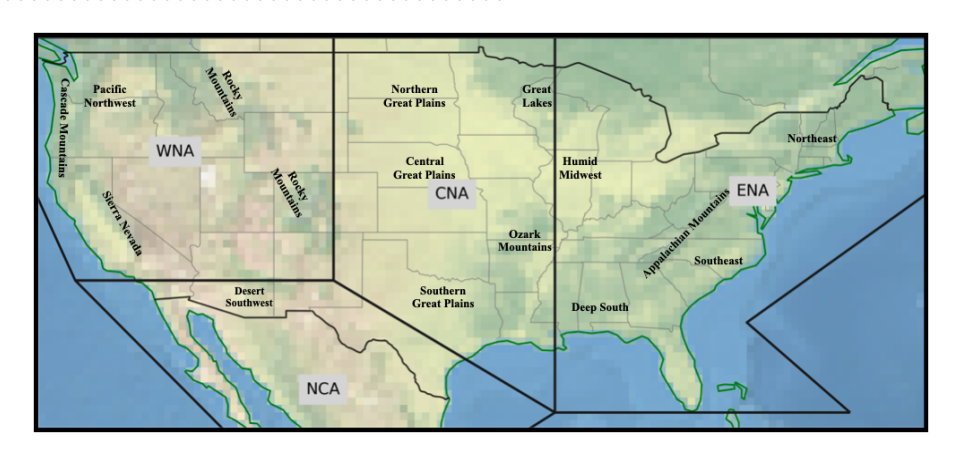


Figure 1. Regional divisions of the CONUS area into four major zones: Western North America (WNA), Central North America (CNA), Eastern North America (ENA), and North Central America (NCA), as defined by Giorgi and Francisco (2000), based on climate variability and geographical features. Prominent subregions and geographical landmarks, such as mountain ranges and plains, are also depicted.

2.2 Data Description

130

135

The Soil Parameter Intercomparison Project (SP-MIP), initiated at the GEWEX-SoilWat workshop in Leipzig (2016), aims to quantify the variability in land surface model (LSM) output caused by differences in soil parameters and structures. Following the Land Surface, Snow, and Soil Moisture Model Intercomparison Project (LS3MIP) protocol (Van den Hurk et al., 2016), SP-MIP brought together eight leading climate land models CLM5, ISBA, JSBACH, JULES, MATSIRO, MATSIRO-GW, NOAH-MP, and ORCHIDEE for a series of global simulation experiments (Gundmundsson and Cuntz, 2017). These models were run on a 0.5° grid using Global Soil Wetness Project Phase 3 (GSWP3) meteorological forcing data for 1980 to 2010. Four experimental designs were implemented to isolate the effects of soil properties on hydrological and energy balance variables. Soil parameters for Experiment 1 and soil textures for Experiment 2 (EXP2) were derived at a 0.5° resolution, based on dominant soil classifications within the 0-5 cm layer of SoilGrids data (Hengl et al., 2014) at a 5 km resolution. The Brooks and Corey parameters are derived from Table 1 of Clapp and Hornberger (1978), while the Mualem-van Genuchten parameters represent ROSETTA class average hydraulic values as cited by Schaap et al. (2001), with soil textures taken from Table 1 of Cosby et al. (1984). For Experiments 4a-d (EXP4a-4d), the USDA soil categories used are Loamy Sand, Loam, Silt,

and Clay, as defined by Montzka et al. (2011), employing identical transfer functions for Brooks and Corey and Mualem-van Genuchten parameters as applied in Experiment 1 (EXP1). All models are assumed to solve the Richards equation for soil water movement. The provided soil parameters and textures are uniform throughout the entire soil column. For a detailed description of the SP-MIP dataset, please refer to (Gundmundsson and Cuntz, 2017).

This study uses soil moisture data from the CLM5 experiments developed by the National Center for Atmospheric Research (NCAR) (Thornton, 2010; Lawrence et al., 2019). The schematic (Figure 2) illustrates the CLM5 modeling framework, depicting the experimental setup for seven different model runs, each designed to evaluate the influence of soil hydraulic parameterizations on soil moisture variability. The dataset covers global landmasses at 0.5° resolution (25,920 grid cells, excluding water bodies and permanent snow/ice) and includes 41 land surface variables such as evapotranspiration, soil temperature, and runoff, spanning 30 years (1980 to 2010). The global soil profile reaches a depth of 41.998 m with 25 layers, but for this study, soil moisture was extracted from depths (0-1.0 m) containing most roots (root zone) of the CONUS region, covering 6,413 grid cells. The focus is on the variable water content of soil layers (mrsol) to explore soil moisture variability and distribution. Importantly, irrigation processes were not represented in any of the CLM5 simulations, as all experiments were conducted under naturalized (rainfed) conditions to isolate the influence of soil hydraulic parameterizations without additional anthropogenic water inputs.

2.2.1 Experimental Designs

145

155

160

165

170

To assess the influence of soil hydraulic parameterizations on soil moisture variability within the CLM5, a series of simulations was conducted following the SP-MIP framework (Gundmundsson and Cuntz, 2017). Although SP-MIP was designed for multi-model comparisons, we adapted it to evaluate intra-model variability within CLM5 by varying soil hydraulic parameter sets. All simulations used consistent meteorological forcing (GSWP3), spatial resolution (0.5°), and spanned 1980 to 2010, with a standardized spin-up routine to ensure reliable initial conditions. Below, we describe the four experimental setups, their objectives, configurations, hypotheses, and expected outcomes, focusing on how parameters are applied within CLM5. Each experiment followed the standard CLM5 spin-up procedure to ensure that carbon, water, and energy state variables reached quasi-equilibrium prior to the simulation period, thereby minimizing the influence of initial conditions on soil moisture dynamics (Lawrence et al., 2019). Spin-up followed SP-MIP protocol guidelines to ensure equilibrium prior to the 1980 to 2010 simulation period (Gundmundsson and Cuntz, 2017).

(1) EXP1: A baseline control was conducted using globally standardized EXP1 – Soil Hydraulic Parameters Provided by SP-MIP: This experiment serves as a baseline simulation, applying soil hydraulic parameters from provided by SP-MIP (refer to Table 1)to examine the presumed decrease in inter-model variability when uniform soil parameters are employed. These parameters, derived from PTFs such as Brooks and Corey (Clapp and Hornberger, 1978) and Mualem-van Genuchten (Schaap et al., 2001), are applied uniformly across all grid cells in the CONUS at a 0.5° resolution using GSWP3 meteorological forcing data (1980 to 2010). The objective is to establish a reference for soil moisture predictions by eliminating spatial variability in soil properties, allowing isolation of CLM5's response to a

consistent soil parameter set. The hypothesis is that SP-MIP soil hydraulic parameters will produce uniform soil moisture patterns, serving as a control to quantify the effects of parameter variations in other experiments. The expected outcome is a consistent baseline for intra-model comparisons, highlighting CLM5's sensitivity to parameter changes rather than inter-model differences.

180

185

200

- (2) EXP2: Soil texture properties provided by SP-MIP (see EXP2 Texture-Derived Soil Hydraulic Parameters: In this experiment, CLM5 uses SP-MIP-provided soil texture inputs (Table 2)utilized lookup tablesor PFTs to determine hydraulic parameters, analyzing the variability caused by parameter translation methods. , such as fractions of clay, silt, sand, dry bulk density, and organic matter content, to derive soil hydraulic parameters internally via its native PTFs and lookup tables. These parameters vary spatially across the CONUS domain based on textural classes. The objective is to assess how CLM5's standard approach to translating soil texture into hydraulic properties influences soil moisture outputs. The hypothesis is that spatial variability in texture-derived parameters will introduce heterogeneity in soil moisture patterns, reflecting CLM5's default parameterization practices. The expected outcome is a simulation that mirrors operational CLM5 runs, enabling comparison with EXP1 to evaluate the impact of texture-to-parameter translation on hydrological variability.
- (3) EXP3: The model applied its EXP3 CLM5 Default Configuration: This experiment employs CLM5's default soil hydraulic settings, maintaining consistent soil properties throughout all layers to explore the intrinsic inter-model variability —parameters, as defined by its operational input datasets, applied consistently across all soil layers throughout the CONUS domain. Unlike EXP1's standardized parameters or EXP2's texture-derived parameters. EXP3 reflects CLM5's inherent configuration without external constraints. The objective is to evaluate the model's intrinsic variability due to its standard soil parameter settings, providing a benchmark for CLM5's default behavior. The hypothesis is that CLM5's default parameters, which vary spatially based on its native soil maps, will produce distinct soil moisture patterns compared to the controlled setups in EXP1 and EXP2. The expected outcome is a simulation that highlights the influence of CLM5's built-in assumptions on soil moisture, allowing quantification of parameter-driven variability within a single model.
 - (4) EXP4a-4d Uniform Soil Texture Simulations: These four experiments (EXP4a-4d: These experiments utilized key : loamy sand, EXP4b: loam, EXP4c: clay, EXP4d: silt) each involve a separate CLM5 simulation with uniform soil hydraulic parameters sourced from SP-MIP (refer to Table 1), employing uniform parametersacross four different soil eategories: loam, clay, silt, and loamy sand. This configuration explored how sensitive LSMs are to soil hydraulic parameters and the impact on spatial variability in both hydrological applied across the entire CONUS domain. The parameters, derived from PTFs for each USDA soil class (Montzka et al., 2011), are spatially constant within each experiment but differ across the four runs based on soil type. The objective is to test CLM5's sensitivity to distinct soil textures and their associated hydraulic properties, such as porosity, saturated hydraulic conductivity, and water retention curves, and to evaluate their impact on hydrological (e.g., soil moisture) and energy balance outputs. (e.g., evapotranspiration) outputs. The hypothesis is that each soil type will produce unique soil moisture patterns, reflecting

texture-dependent hydrological behavior. The expected outcome is a set of simulations that isolate the effects of soil texture on CLM5's outputs, providing insights into parameter-driven variability across diverse soil types.

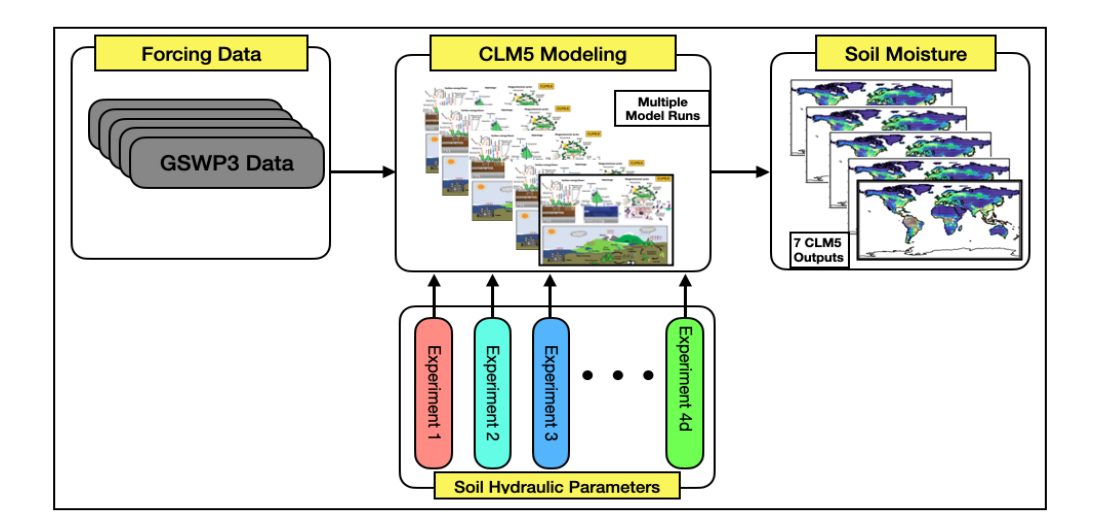


Figure 2. Experimental setup for evaluating soil moisture variability in CLM5. The model uses GSWP3 forcing data and runs multiple experiments with different soil hydraulic parameterizations. EXP1 applies standardized parameters, EXP2 derives parameters from soil texture, EXP3 uses default CLM5 settings, and EXP4a–4d assign uniform parameters for different soil types.

210 2.2.2 Benchmark Reference Dataset

215

220

225

The ERA5-Land dataset, provided by the European Centre for Medium-Range Weather Forecasts (ECMWF), serves as a key reference for model evaluation. Unlike other models, ERA5-Land does not directly incorporate soil moisture observations. Instead, it uses atmospheric data from the ERA5 reanalysis, which integrates meteorological and satellite observations via a 4-D variational assimilation system coupled with a simplified extended Kalman filter (Muñoz-Sabater et al., 2021). This methodology enables land surface changes to be primarily guided by modeled processes while being affected by larger atmospheric conditions. In terms of soil moisture, the ERA5 system assimilates information from a range of satellite sources, such as the Soil Moisture Ocean Salinity (SMOS), Advanced Microwave Scanning Radiometer-2 (AMSR-2), Tropical Rainfall Measuring Mission Microwave Imager (TRMM-MI), ERS-1/2 Active Microwave Instrument scatterometer, and Meteorological Operational Satellite (De Rosnay et al., 2013). Although ERA5-Land uses an indirect method for assimilation, it is often employed as a reference for validating soil moisture data due to its global consistency and frequent updates. However, studies have pointed out certain discrepancies, like a wet bias in its soil moisture measurements relative to ground-based and SMAP-Soil Moisture Active Passive (SMAP) satellite data, especially in heavily vegetated and humid areas (Lal et al., 2022). Additionally, ERA5-Land does not account for anthropogenic water management such as irrigation, which can significantly affect soil moisture levels in intensively cultivated regions. As documented in previous studies, the absence of irrigation in the H-TESSEL land surface model used by ERA5-Land has been linked to underestimation of soil moisture in irrigated areas and is a known limitation when

Table 1. Soil parameters for the three selected water retention curves were supplied by SP-MIP as input for experiments 1 and 4a-d.

Parameter Name	long_name (netCDF)	<u>Unit</u>
<u>he</u>	air entry potential	$\stackrel{\mathbf{m}}{\sim}$
mbc_	Brooks-Corey m parameter = Clapp-Hornberger b	≂
thetar	residual soil moisture	$\underbrace{\text{m}^3 \text{m}^{-3}}_{}$
thetas	saturated soil moisture, porosity	$\underbrace{m^3m^{-3}}_{}$
<u>ks</u>	Hydraulic conductivity at saturation or at air entry	$\underset{\sim}{\text{ms}}^{-1}$
lambdac	Corey lambda parameter	≂
alphavg	van Genuchten alpha parameter	$ \overset{\mathbf{m}^{-1}}{\sim} $
nvg	van Genuchten n parameter	≂
₩vg	van Genuchten m parameter	≂
thetafcbc	Brooks-Corey field capacity	$ \overset{\text{m}^3 \text{ m}^{-3}}{\longrightarrow} $
thetafcvg	van Genuchten field capacity	
thetapwpbc	Brooks-Corey permanent wilting point	$ \overset{\text{m}^3 \text{ m}^{-3}}{\longrightarrow} $
thetapwpvg	van Genuchten permanent wilting point	<u>m³ m⁻³</u>

interpreting results over agricultural landscapes (Wipfler et al., 2011; Lavers et al., 2022; Tang and McColl, 2023). These biases highlight the importance of careful interpretation when applying ERA5-Land to hydrological tasks. Despite these issues, its capacity to reflect broad spatiotemporal patterns ensures its effectiveness in assessing model performance and conducting extensive hydrological research. While alternative datasets such as the North American Land Data Assimilation System (NL-DAS) could provide higher resolution and are region-specific to CONUS, ERA5-Land was selected for its global consistency, frequent updates, and ability to offer a broader perspective that facilitates comparison across varying climatic conditions. Additionally, ERA5-Land provides a direct connection to global atmospheric reanalysis, enabling robust assessments of large-scale interactions between soil moisture and climate processes. The ERA5-Land dataset data was regridded to fit the CLM5 0.5° resolution.

Table 2. Soil textural characteristics supplied by SP-MIP for experiment 2.

Parameter Name	long_name (netCDF)	<u>Unit</u>
<u>fclay</u>	fraction of clay	-
<u>fsilt</u>	fraction of silt	≂
fsand	fraction of sand	≂
rhosoil	dry bulk density	kgm ^{−3}
omsoil	organic matter content	$g(C)kg^{-1}$

Soil parameters for the three selected water retention curves were supplied by SP-MIP as input for experiments 1 and 4a-d.

Parameter Name long_name (netCDF) Unit he air entry potential mmbe Brooks-Corey m parameter = Clapp-Hornberger b

-thetar residual soil moisturem³ m⁻³thetas saturated soil moisture, porositym³ m⁻³ksHydraulic conductivity at saturation or at

air entryms⁻¹lambdacCorey lambda parameter—alphavgvan Genuchten alpha parameterm⁻¹nvgvan Genuchten n parameter—mvgvan

Genuchten m parameter—thetafebeBrooks-Corey field capacitym³ m⁻³thetafevgvan Genuchten field capacitym³ m⁻³thetapwpbeBrooks-C

permanent wilting pointm³ m⁻³thetapwpvgvan Genuchten permanent wilting pointm³ m⁻³

Soil textural characteristics supplied by SP-MIP for experiment 2. Parameter Name long_name (netCDF) Unit felay fraction of clay –fsilt fraction of silt –fsand fraction of sand –rhosoil dry bulk density kgm⁻³omsoil organic matter contentg(C)kg⁻¹

2.3 EOF Analysis for Soil Moisture Variability

250

255

EOF analysis is a well-established statistical technique used widely utilized statistical method in geophysical sciences to reduce the dimensionality of complex datasets while preserving their most significant variability patterns (Jollife, 2002) for extracting dominant spatiotemporal patterns from high-dimensional datasets (Jollife, 2002; Björnsson and Venegas, 1997). Originally introduced in meteorology by Lorenz (1956), it has been widely applied to analyze spatio-temporal variability in by Lorenz (1956) in the context of meteorology, EOF analysis has evolved into a foundational tool for analyzing climate and hydrological systems (Monahan et al., 2009). EOF analysis systematically decomposes large datasets variables such as precipitation, evapotranspiration, and soil moisture (Monahan et al., 2009; Korres et al., 2010). The method works by decomposing a dataset into orthogonal spatial patterns (EOF modesEOFs) and their corresponding temporal ecomponents amplitudes (principal components, PCs) ; enabling the identification of dominant variability modes and their temporal evolutionthrough linear algebra techniques such as Singular Value Decomposition (SVD) (Hannachi et al., 2007; Dawson, 2016). In this study, EOF analysis is applied to soil moisture fields simulated by outputs from the CLM5 across the CONUS region. This approach isolates spatial and temporal patterns domain. The objective is to assess how varying soil hydraulic parameterizations influence both the spatial structure

and temporal evolution of soil moisture-variability, providing insights into the influence of soil hydraulic parameterizations on large-seale moisture distribution and the temporal dynamics of extremes such as particularly in the context of seasonal-to-interannual climate variability and hydrologic extremes like droughts and floods. Previous studies have demonstrated the effectiveness of EOF in linking soil moisture variability to large-seale climate driversEOF analysis is well-suited to this objective because it captures the internal covariance structure of spatial fields and retains dominant modes of variability that simpler diagnostics, such as the El Niño-Southern Oscillation (ENSO) and drought-flood cycles (Bauer-Marschallinger et al., 2013; Korres et al., 2010), highlighting its utility in disentangling the role of parameterization from other drivers (Lorenz, 1956; Jawson and Niemann, 2007). The EOF modes extracted in this study capture dominant spatial patterns RMSE or mean bias, may obscure.

EXP1, EXP3, while the PCs characterize their evolution under varying climate and environmental conditions. This enables the evaluation of parameter-specific impacts, addressing uncertainties associated with EXP4a-4d) and against observational benchmarks like ERA5-Land. This facilitates the detection of parameter-sensitive regions and improves the mechanistic understanding of how soil hydraulic properties and their role in controlling soilmoisture variability. While EOF analysis effectively reveals statistical patterns, its results must be interpreted cautiously, as modes are mathematical constructs that may not directly correspond to modulate model behavior. Such insights are particularly valuable in hydroclimatically complex regions, including the central Great Plains and the arid western U.S., where soil-climate interactions display high spatial heterogeneity. Moreover, EOF techniques have proven effective for diagnosing how land surface processes, especially soil moisture dynamics, interact with large-scale atmospheric teleconnections such as ENSO, the Pacific Decadal Oscillation (PDO), and the North Atlantic Oscillation (NAO) (Jimma et al., 2023; Kuss and Gurdak, 2014). In this context, EOFs help reveal persistent spatiotemporal modes and teleconnection pathways that underlie soil moisture memory and seasonal predictability (Orth and Seneviratne, 2012; Perry and Niemann, 2007). These properties support both model evaluation and the interpretation of hydroclimatic variability from a process-oriented perspective.

However, care must be taken in interpreting EOF results. The orthogonality constraint can produce modes that are statistically optimal but not necessarily tied to discrete physical processes (Hannachi et al., 2007). The identified patterns serve as a basis for further analysis, supporting model calibration and validation efforts to enhance the predictive capabilities of LSMs. To facilitate this analysis, this research employs a Python library for EOF analysis of meteorological, oceanographic, and elimate data developed by Dawson (2016) To address this limitation, our study complements EOF analysis with additional diagnostics—such as Euclidean distance metrics and Taylor diagrams—to evaluate spatial pattern fidelity and the sensitivity of model output to parameter perturbations. All EOF analyses are performed using the open-source Python package eofs (Dawson, 2016), which is optimized for climate and Earth system data. This ensures a reproducible, efficient, and physically interpretable workflow for quantifying parameter-driven variability in land surface model simulations.

2.3.1 Computation of EOF Using Singular Value Decomposition

260

265

270

275

280

285

Singular Value Decomposition (SVD) is a robust linear algebra technique widely employed for matrix factorization, enabling the decomposition of any $n \times m$ matrix, \mathbf{Y}_m , without explicitly solving an eigenvalue problem or constructing a covariance

matrix (e.g., Linz and Wang, 2003; Dawson, 2016; Björnsson and Venegas, 1997). In this study, SVD is utilized to compute the EOF modes by decomposing the matrix of soil moisture anomalies, \mathbf{Y}_w , into orthogonal components. The decomposition is represented as:

$$\begin{bmatrix} \mathbf{Y}_{w} : \\ n \times m \end{bmatrix} = \begin{bmatrix} u_{11} & u_{12} & \cdots & u_{1p} \\ u_{21} & u_{22} & \cdots & u_{2p} \\ \vdots & \vdots & \ddots & \vdots \\ u_{n1} & u_{n2} & \cdots & u_{nn} \end{bmatrix} \begin{bmatrix} \gamma_{11} & 0 & \cdots & 0 \\ 0 & \gamma_{22} & \cdots & 0 \\ \vdots & \vdots & \ddots & \vdots \\ 0 & 0 & \cdots & \gamma_{nm} \end{bmatrix} \begin{bmatrix} v_{11} & v_{12} & \cdots & v_{1p} \\ v_{21} & v_{22} & \cdots & v_{2p} \\ \vdots & \vdots & \ddots & \vdots \\ v_{n1} & v_{n2} & \cdots & v_{nm} \end{bmatrix}$$
(1)

$$\mathbf{Y}_{w} = \mathbf{U}\boldsymbol{\Gamma}\mathbf{V}^{T},\tag{2}$$

where \mathbf{U} $(n \times n)$ contains the left singular vectors (spatial EOFs), \mathbf{V} $(m \times m)$ contains the right singular vectors (temporal principal components, PCs), and $\mathbf{\Gamma}$ $(n \times m)$ is a diagonal matrix with non-negative singular values γ_i $(\Gamma_{ij} = \delta_{ij}\gamma_i)$. The singular values γ_i quantify the variance captured by each EOF mode, and $\rho = \min(n, m)$ determines the number of non-zero singular values.

For this analysis, the soil moisture data matrix Y_w represents the consists of area-weighted, demeaned anomalies anomaly values simulated by CLM5, with where the mean at each grid point has been removed to highlight variability. The matrix has n rows corresponding to temporal representing time steps and m columns representing corresponding to spatial grid points. To reduce redundancy, we employ and focus on the most significant patterns, we apply truncated SVD (tSVD), retaining only the top ρ singular values and their associated corresponding singular vectors:

305
$$\mathbf{Y}_w \approx \hat{\mathbf{U}}_{\rho} \hat{\mathbf{\Gamma}}_{\rho} \hat{\mathbf{V}}_{\rho}^T,$$
 (3)

where $\hat{\mathbf{U}}_{\rho}$ $(n \times \rho)$ contains the leading EOFs, $\hat{\mathbf{\Gamma}}_{\rho}$ $(\rho \times \rho)$ is the diagonal matrix of the largest singular values, and $\hat{\mathbf{V}}_{\rho}^{T}$ $(\rho \times m)$ represents the corresponding principal components. Singular vectors associated with smaller singular values are discarded, improving computational efficiency while preserving the dominant variability patterns (Figure 3).

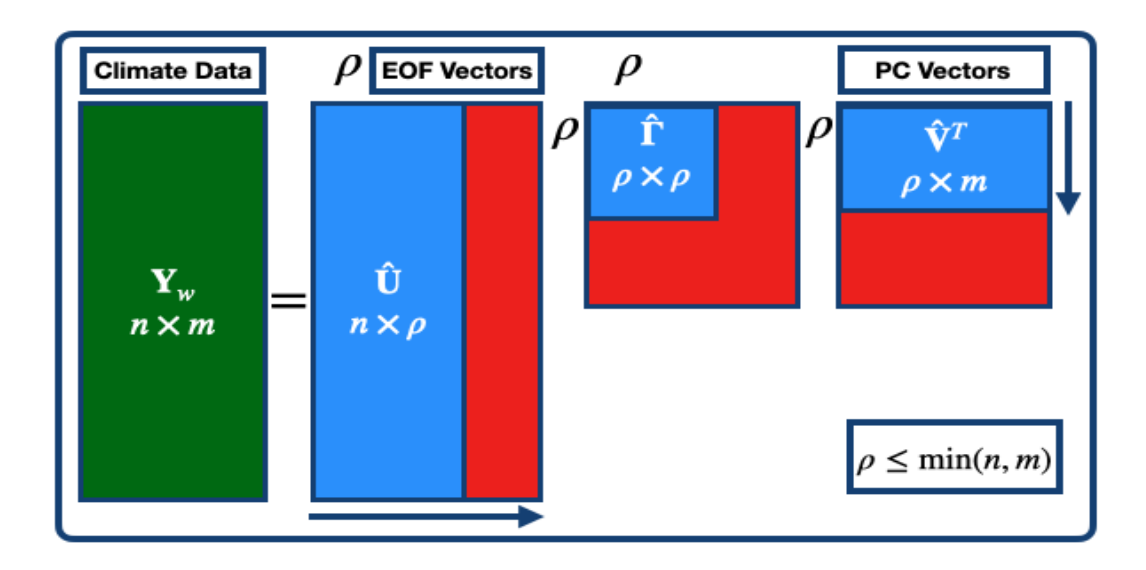


Figure 3. tSVD applied to the soil moisture anomaly dataset. The matrix \mathbf{Y}_w $(n \times m)$ is decomposed into $\hat{\mathbf{U}}_\rho$ $(n \times \rho)$ for EOFs, $\hat{\mathbf{\Gamma}}_\rho$ $(\rho \times \rho)$ for singular values, and $\hat{\mathbf{V}}_\rho^T$ $(\rho \times m)$ for PCs. The truncation level ρ is chosen such that $\rho \leq \min(n, m)$.

The singular values from tSVD are used to calculate the explained variance (%EV $_i$) for each EOF mode, quantifying their contribution to the dataset's variability:

$$\%EV_{i} = \frac{\gamma_{i}}{\sum_{j=1}^{\rho} \gamma_{j}} \times 100\%, \quad i = 1, 2, \dots, \rho.$$
(4)

The first EOF mode typically explains the largest fraction of variance, representing the dominant spatial pattern, while subsequent modes capture progressively smaller uncorrelated patterns. This hierarchical decomposition provides a powerful framework for analyzing spatiotemporal variability in soil moisture anomalies and assessing the relative contributions of soil hydraulic parameters and climate drivers. EOF analysis, through tSVD, ensures that the representation of dominant patterns is efficient and interpretable, enabling robust physical insights into the factors controlling soil moisture variability.

2.3.2 Quantifying Similarity of Spatial EOF Modes Using using Euclidean Distance

315

320

The Euclidean distance metric was employed to assess the similarity or dissimilarity between spatial EOF modes derived from distinct datasets. This metric, commonly used in mathematics and data analysis, calculates the straight-line distance between two points in Euclidean space, providing a direct and interpretable measure of the geometric proximity between patterns (e.g., Elmore and Richman, 2001). Its simplicity and intuitive interpretation make it particularly suitable for comparing spatial variability patterns obtained through EOF analysis. A smaller Euclidean distance indicates a high degree of similarity between the EOF modes, suggesting a closer alignment of the underlying spatial patterns. Conversely, a larger distance reflects greater dissimilarity, indicating distinct spatial characteristics or variability between the datasets. In this study, the Euclidean distance

was used to compare the spatial EOF modes from the ERA5-Land reanalysis dataset and the SP-MIP model experiments, representing different data decomposition results. The Euclidean distance for two spatial EOF modes, \mathcal{X} (ERA5-Land) and \mathcal{Y} (SP-MIP), was computed using the following equation:

$$\operatorname{EucD}(\mathcal{X}, \mathcal{Y}) = \sqrt{\sum_{i=1}^{n} (\mathcal{X}_i - \mathcal{Y}_i)^2},$$
(5)

where n is the number of elements in each spatial EOF mode.

This approach enabled the identification of regions within the CONUS domain where the spatial EOF patterns differed significantly, highlighting areas requiring improved parameterization of soil properties in land surface models LSMs. By quantifying these differences, the Euclidean distance analysis provides actionable insights into the spatial scales and regions where soil parameter settings have the most significant impact, thereby supporting targeted model refinements and enhanced soil moisture simulations.

2.3.3 Taylor Diagram for Evaluating Spatial EOF Modes

Taylor Diagrams (TDs) (Taylor, 2001) were applied to assess spatial EOF modes, offering a clear and intuitive visualization of three essential statistical measures: correlation (COR), standard deviation (STD), and root mean square error (RMSE). These diagrams are extensively employed in geophysical sciences to evaluate and compare model performance across various dimensions (e.g., Qiao et al., 2022). Their capability to display the relationship between modeled and observed patterns simultaneously makes them particularly useful for examining the variability and accuracy of spatial EOF modes derived from climate datasets. In this research, Taylor diagrams were used to compare the spatial EOF modes of the ERA5-Land reanalysis dataset against the SP-MIP model experiments. The standard deviation of the ERA5-Land spatial modes served as a benchmark for assessing the variability of the SP-MIP modes. The diagrams assessed the similarity of the patterns by using three metrics: the correlation coefficient, which evaluates the alignment of spatial patterns; the centered RMSE, which measures the magnitude of pattern differences; and the standard deviation, which indicates the amplitude of variability within each mode. These combined metrics offer a thorough assessment of spatial pattern differences. Taylor diagrams help identify specific EOF modes where SP-MIP experiments differ from the ERA5-Land reference, pinpointing areas for possible model enhancement. By incorporating these metrics into one framework, the diagrams facilitate the focused improvement of soil parameterizations in land surface models LSMs, better capturing essential spatial variability patterns in soil moisture.

350 3 Results and Discussion

330

335

340

345

3.1 Spatial Variability in Annual Mean Soil Moisture Across CONUS

Despite consistent forcing data (GSWP3) and model resolution (0.5°), the experiments reveal notable differences in soil moisture spatial patterns due to variations in soil parameter derivation, underscoring the critical role of soil parameters in controlling simulations. These differences are reflected in the annual mean soil moisture across the CONUS region, which ranged from

≈ 195kg m⁻² to 380kg m⁻², calculated by averaging daily soil moisture from 1980 to 2010 (Figure 4). The spatial distribution of soil moisture across all experiments reflects well-established precipitation gradients and temperature variability, with higher soil moisture levels over the central Great Plains and ENA regions and lower values in the arid southwest (WNA). These findings agree with previous studies documenting the relationship between soil moisture, precipitation, and temperature in these regions (Welty and Zeng, 2018; Koster et al., 2004; Koukoula et al., 2021; Melillo et al., 2014; Chatterjee et al., 2022).
 The pronounced variability in soil moisture in the Great Plains aligns with the principles of continentality, where greater distances from large water bodies amplify seasonal precipitation and evaporation differences (Gimeno et al., 2010). Among the experiments, EXP3 (Figure 3d) shows the highest soil moisture levels, followed by EXP2 (Figure 4c) and EXP1 (Figure 4b). These differences reflect the impact of soil parameter derivation, with EXP1 producing lower soil moisture magnitudes, EXP2 resulting in moderate values, and EXP3 yielding the highest levels.

365

370

375

380

The results of EXP4 highlight the role of soil texture in modulating soil moisture distribution. For example, EXP4a (loamy sand, Figure 4e) exhibits low soil moisture in the arid southwest (WNA) and NCA, consistent with the limited water retention capacity of loamy sand. EXP4b (loam, Figure 4f) shows a more balanced soil moisture distribution, with drier conditions in WNA and wetter conditions in ENA, reflecting the moderate water holding characteristics of the loam. EXP4c (clay, Figure 4g) shows higher soil moisture levels over ENA due to the high water retention capacity of clay, while EXP4d (silt, Figure 4h) exhibits heterogeneous soil moisture patterns influenced by environmental variability and the intermediate hydraulic properties of the silt. These results show that uncertainties in soil parameterization significantly affect soil moisture simulations in the CLM5 model, consistent with the findings of Brimelow et al. (2010). Our work furthers this research area by systematically evaluating the role of distinct soil textures (loamy sand, loam, clay, and silt) in shaping soil moisture variability across different climatic zones. Unlike previous studies, this analysis integrates the spatial distribution of soil moisture with observed climatic influences, providing a more comprehensive assessment of how parameterization impacts hydrological processes at a continental scale. Variations in soil parameter settings not only influence soil moisture magnitudes but also alter spatial distributions, affecting the model's ability to capture hydrological processes at the continental scale. The findings of EXP4 further emphasize the importance of soil texture in controlling soil moisture distribution, highlighting the need for precise parameterization in land surface models LSMs. This has important implications for improving water resource management, agricultural planning, and climate impact assessments.

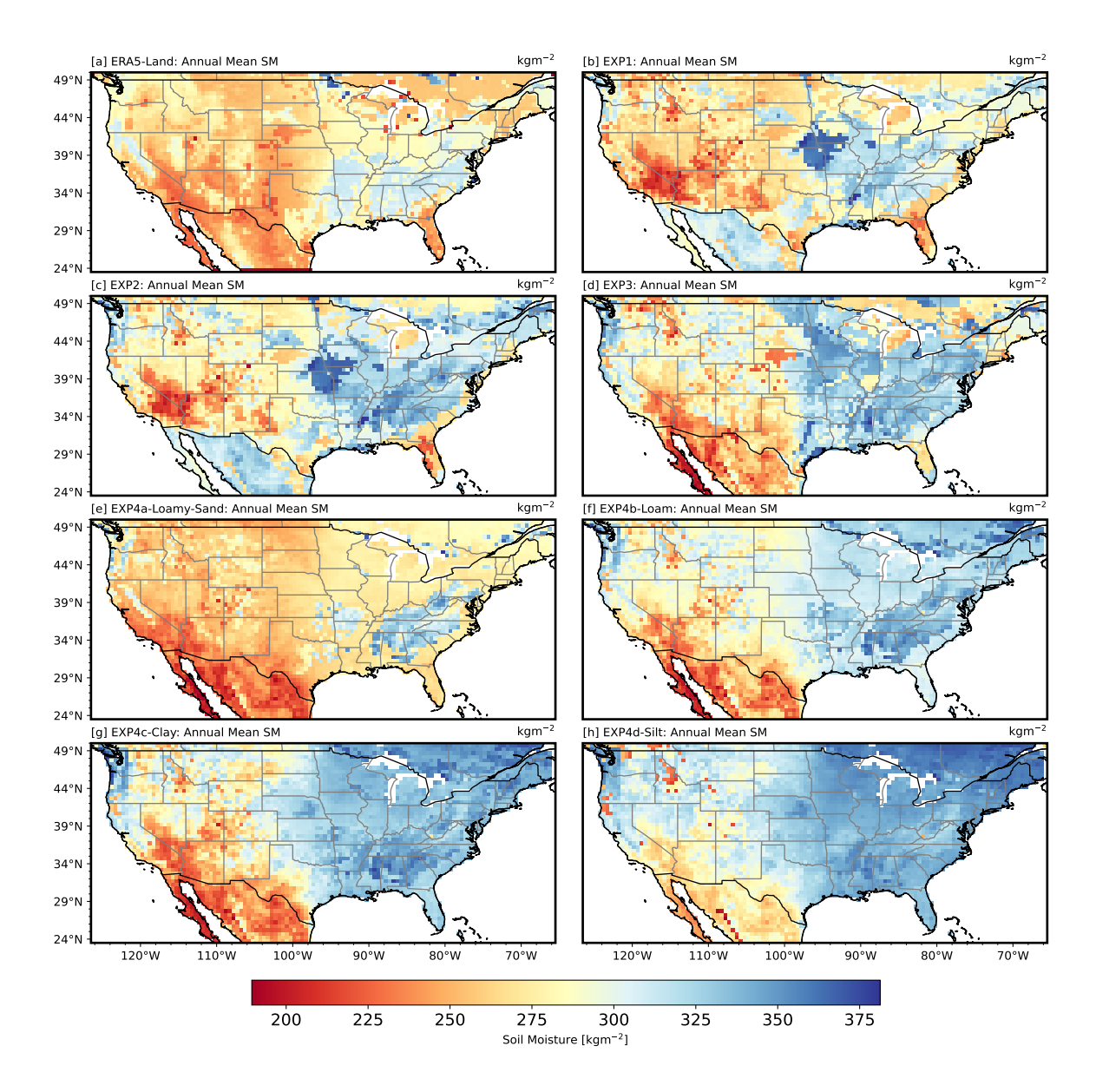


Figure 4. Annual mean soil moisture (1980–2010) over the CONUS region, simulated from four experiment types with spatially uniform soil parameter settings: EXP1 (b), EXP2 (c), EXP3 (d), and EXP4 (sub-experiments: EXP4a: loamy sand (e), EXP4b: loam (f), EXP4c: clay (g), and EXP4d: silt (h)). The color bar represents the range of soil moisture values (kg m⁻²), with warmer colors (red and orange) indicating lower soil moisture levels and cooler colors (blue and purple) representing higher soil moisture levels.

3.2 Interannual Soil Moisture Anomalies

Interannual root-zone soil moisture anomalies over the CONUS region from 1980 to 2010, derived from CLM5 simulation experiments (EXP1, EXP2, EXP3, and multiple EXP4 configurations) and ERA5-Land reanalysis data, are shown in Figure 5.

Anomalies are computed as deviations from the daily annual mean over the 30-year reference period, following established methodologies for hydrological variability assessment (Tuttle and Salvucci, 2016; Koster et al., 2004; Welty and Zeng, 2018). The top panel of Figure 5 presents anomalies for EXP1, EXP2, EXP3, and ERA5-Land, while the bottom panel includes additional EXP4 parameterizations representing different soil textures (loamy sand, loam, clay, and silt).

Across all configurations, soil moisture anomalies fluctuate around a long-term mean of zero, with values ranging approximately from -20kg m^{-2} to $+40 \text{kg m}^{-2}$. Positive anomalies signify wetter-than-average conditions, while negative values indicate drier conditions. The CLM5 experiments exhibit pronounced interannual variability, capturing key hydrological extremes, including droughts and wet periods, as observed in ERA5-Land. Notably, CLM5 simulations reproduce the timing of major interannual features observed in ERA5-Land, such as drought and wet periods, but consistently underestimate their magnitude. As shown in Figure 5, all CLM5 configurations produce tightly clustered time series, lacking the broader spread of ERA5-Landanomalies show higher peaks, particularly in positive extremes, suggesting a possible overestimation. This visual clustering illustrates a key discrepancy: ERA5-Land exhibits a broader interannual amplitude, with anomalies reaching up to $\pm 40 \text{kg m}^{-2}$, whereas CLM5 simulations are typically confined to a $\pm 20 \text{kg m}^{-2}$ range.

This variability gap likely stems from structural limitations in CLM5, including the use of static soil hydraulic parameters, diffusive vertical redistribution, and the absence of data assimilation—factors known to constrain the dynamic range and persistence of soil moisture anomalies in LSMs (Koster et al., 2009; Muñoz-Sabater et al., 2021). The underestimation is particularly concerning for hydrologic extremes, as it suggests that CLM5 may inadequately simulate the severity of soil moisture in heavily vegetated regions (Lal et al., 2022). Despite these discrepancies, the time-series plots reveal a broad agreement between deficits during droughts or surpluses during wet years. These limitations can propagate into downstream processes such as evapotranspiration, runoff, and land—atmosphere coupling, thereby reducing the model's ability to capture feedback mechanisms critical to hydroclimatic variability (Koster et al., 2004; Berg and Sheffield, 2018). Figure 6 supports this interpretation, showing that CLM5 simulations and reanalysis data in terms of both seasonal and interannual variability, anomaly values are compressed along the 1:1 line when compared to ERA5-Land, reinforcing the conclusion that the model's soil moisture response is systematically dampened. Finally, while ERA5-Land's higher peaks—particularly in positive extremes—may partly reflect overestimation in vegetated regions due to unresolved processes such as irrigation or enhanced surface fluxes (Lal et al., 2022), the muted variability in CLM5 highlights the importance of improved parameter calibration and multi-source observational benchmarking in future work.

The relationship between daily soil moisture anomalies from CLM5 and ERA5-Land is further examined in Figure 6. These scatter plots compare CLM5-simulated anomalies with ERA5-Land on a point-by-point basis. The distribution of points is closely aligned along the 1:1 line, with coefficient of determination (R^2) values ranging from 0.7 to 0.8 across experiments. These correlations confirm that CLM5 successfully captures the overall variability in ERA5-Land, albeit with some systematic biases. Specifically, ERA5-Land tends to exhibit larger positive anomalies relative to CLM5, reinforcing the trend observed in the time-series plots. The EXP4 configurations (Figure 6b) show similar performance to EXP1-3, indicating that soil texture variations only moderately impact anomaly correlations at an aggregated scale.

The results indicate significant interannual variability in soil moisture anomalies, with distinct peaks and troughs corresponding to extreme hydrological events. These fluctuations are likely driven by large-scale climatic influences, such as ENSO, which modulate regional hydrological conditions (Gimeno et al., 2010; Welty and Zeng, 2018). While periodicity in anomalies suggests a possible linkage to climate oscillations, further spectral analysis would be required to confirm such relationships. Additionally, the lack of a discernible long-term trend suggests that soil moisture anomalies remained relatively stable over the study period, with variability largely governed by short to medium-term hydrological cycles. This aligns with findings from Lesinger and Tian (2022), who noted that while interannual fluctuations in soil moisture can be significant, multi-decadal trends over CONUS tend to be weak or spatially constrained. Overall, the time-series (Figure 5) and scatter plots (Figure 6) collectively demonstrate that CLM5 accurately simulates reasonably captures the timing and structure of interannual soil moisture variability in CONUS, but consistently underestimates its magnitude relative to ERA5-Land, with strong correlations to ERA5-Land. However, ERA5-Land's systematic overestimation of positive anomalies highlights a potential bias in reanalysis products, necessitating further evaluation of the mechanisms driving such deviations. Future work should assess regional patterns in soil moisture dynamics and quantify biases across different land cover types to refine model performance.

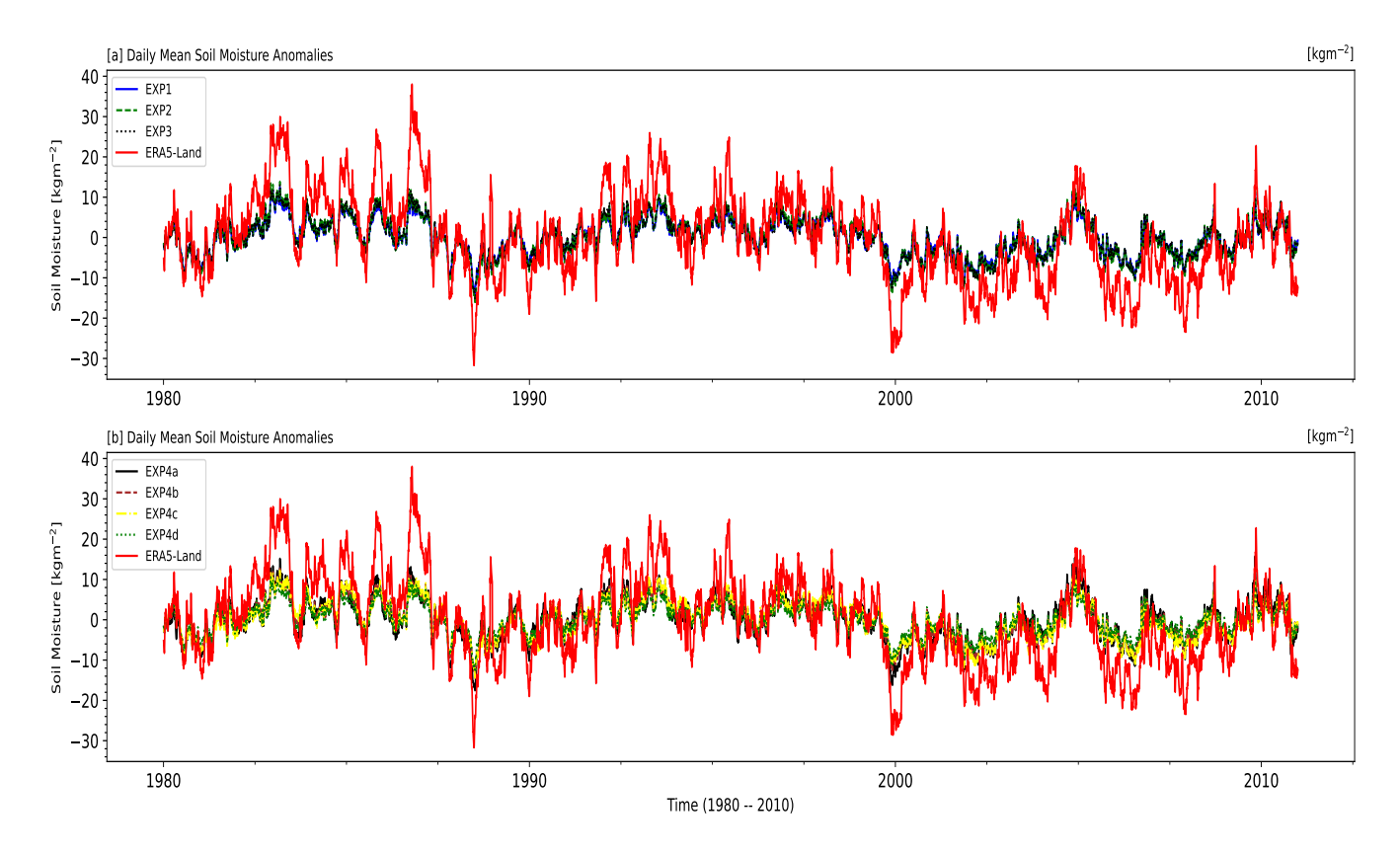


Figure 5. Daily—Time series of daily root-zone soil moisture anomalies from 1980 to 2010 across—over the CONUS region. Panel (a) Anomalies shows anomalies for CLM5 simulations using EXP1, EXP2, EXP3, and EXP3 configurations compared with ERA5-Landdata. Panel (b) Anomalies for various includes EXP4 configurations simulations with uniform soil texture classes (loamy sand, loam, clay, and silt) alongside—, also compared against ERA5-Landdata. Anomalies are calculated computed as deviations from the 30-year daily annual climatological meanover the 30-year period. ERA5-Land exhibits a wider anomaly range, while CLM5 simulations show more constrained variability, highlighting differences in interannual amplitude across configurations.

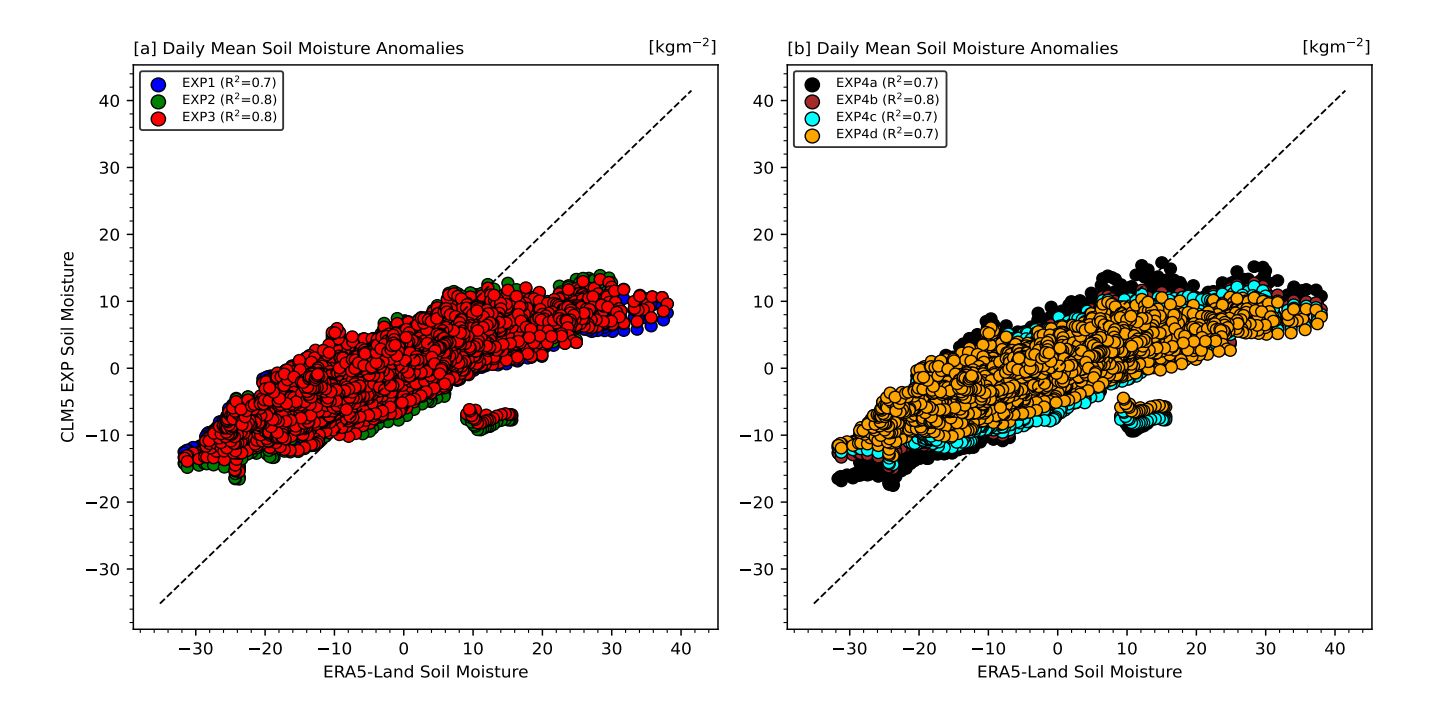


Figure 6. Daily mean root-zone soil moisture anomalies for 1980 to 2010 from each CLM5 experiment (EXP1, EXP2, EXP3, and the EXP4 sub-experiments) plotted against ERA5-Land. All anomalies are expressed in $[kg m^{-2}]$. Each colored marker represents daily anomalies from a given experiment, while the black dashed line denotes the 1:1 relationship. In the legend, R^2 values (in parentheses) indicate how closely each experiment's anomalies match those of ERA5-Land.

3.3 Seasonal Variability of Soil Moisture

435

440

Seasonal cycles of monthly mean soil moisture over the CONUS (1980–2010), comparing As evident in Figure 7, significant differences emerge between ERA5-Land and CLM5 simulations(, particularly in the amplitude of seasonal variability. ERA5-Land exhibits the strongest seasonal cycle, with a sharp rise in soil moisture from February through May, peaking in June, followed by a pronounced decline into the late summer and early autumn months. In contrast, EXP1–, EXP2, and EXP3 and various EXP4 configurations) with ERA5-Land reanalysis (Figure 7). All models and ERA5-Land exhibit coherent seasonal patterns, characterized by winter maxima and summer minima, aligning with the seasonal interplay of precipitation and evapotranspiration dynamics. These trends are consistent with earlier evaluations of CMIP5 soil moisture simulations (Yuan and Quiring, 2017). Notable inter-experiment discrepancies emerge in the amplitude and phasing of soil moisture variability. For exampleform a tightly clustered group with relatively flattened seasonal curves. These configurations consistently underestimate the springtime peak and summer drawdown, suggesting that their soil moisture response to seasonal climate forcing is muted. Among them, EXP2 (green line) shows the lowest amplitude, while EXP3 (red line) offers a slightly improved but still subdued representation.

Notably, EXP4a (loamy sand) displays pronounced springtime fluctuations due to its low water retention capacity, amplifying responses black dashed line) deviates from this pattern. It more closely mirrors ERA5-Land's seasonal dynamics, especially from March to September, capturing a steeper ascent in spring and a deeper trough in late summer. This improved responsiveness is likely due to the loamy sand texture used in EXP4a, which promotes rapid infiltration and drainage, thereby amplifying soil moisture variability in response to precipitation and evapotranspiration. Conversely, EXP4e (clay) and In contrast, EXP4b-d (loam, clay, silt) progressively dampen the seasonal signal, with EXP4c and EXP4d (silt) exhibit dampened seasonal variability, reflecting their greater water retention efficiency. Systematic biases are evident across experiments: winter and spring soil moisture is underestimated relative to showing the lowest variability due to their high water retention capacities.

445

450

455

460

465

These differences indicate that while CLM5 is able to reproduce the general phasing of the seasonal cycle, it substantially underrepresents the amplitude of variation observed in ERA5-Land. This underestimation is especially critical during the peak moisture accumulation (March-June) and depletion (July-October) phases, and highlights the importance of hydraulic conductivity, retention characteristics, and vertical redistribution in modulating soil moisture seasonality. Although ERA5-Land , while summer values are overestimated. These mismatches likely stem from inaccuracies in soil hydraulic parameterizations governing infiltration, storage, and drainage processes. Interpretive caution is warranted, however, as ERA5-Land itself carries a documented wet bias compared to in situ observations and SMAP satellite retrievals, particularly in densely vegetated areas. This bias also arises from discrepancies in vertical representation; in situ sensors measure moisture at 5cm depth, whereas ERA5-Land integrates the 0 may overestimate soil moisture in certain vegetated regions (Lal et al., 2022; Lesinger and Tian, 2022) , its higher amplitude suggests a more dynamic land surface response that current CLM5 configurations, particularly EXP1—7em layer, which retains more moisture post-precipitation Lesinger and Tian (2022). Such differences underscore the need to reconcile observational and modeled soil moisture definitions. Despite these challenges, the EXP3 fail to capture adequately, Addressing this discrepancy through improved parameter tuning and structural adjustments could enhance CLM5simulations robustly reproduce the broad seasonal trends observed in ERA5-Land, affirming their utility for large-scale hydrological analysis. The identified biases, however, highlight critical opportunities to refine soil parameterizations particularly hydraulic properties and vertical layering schemes to better align modeled and observed soil moisture dynamics. Addressing these limitations eould enhance the representation of land-atmosphere feedbacks in climate simulations. 's ability to simulate land-atmosphere coupling and surface hydrological processes across seasons.

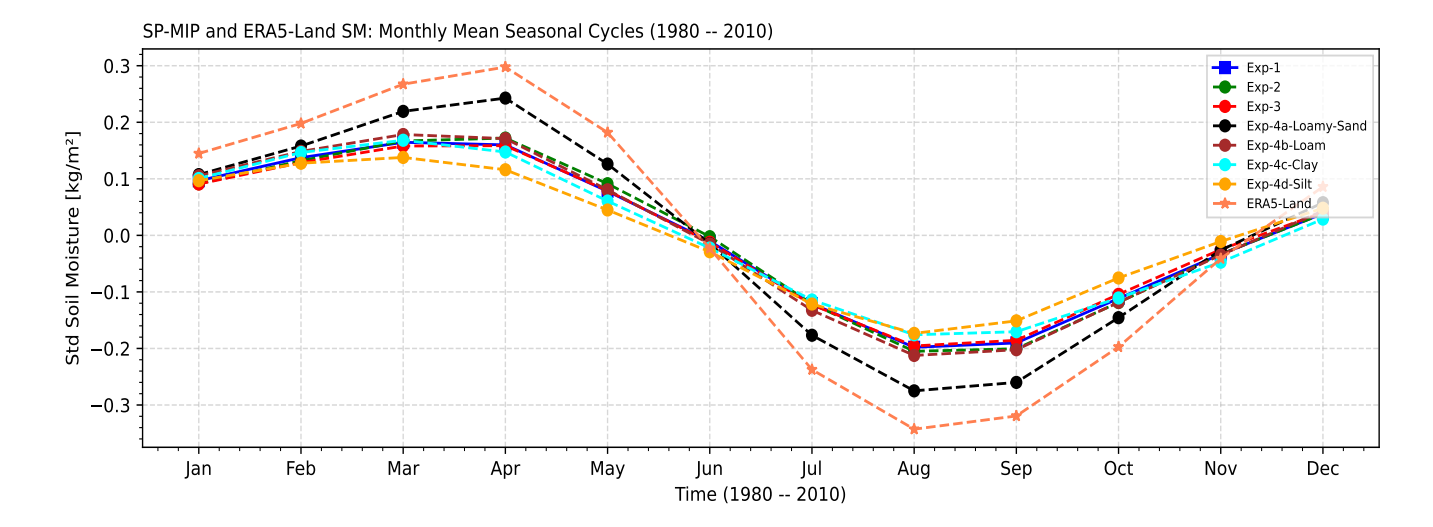


Figure 7. Monthly mean seasonal cycles of standardized root-zone soil moisture for the period 1980–2010, comparing SP-MIP experiments across the CONUS. CLM5 simulations (EXP1, EXP2, EXP3, and various configurations of EXP4EXP4a—d) are compared with ERA5-Land data for reanalysis. ERA5-Land exhibits the CONUS region largest seasonal amplitude, with sharp increases during spring (March—June) and steep declines during summer (July—October). The In contrast, EXP1–EXP3 form a tightly clustered group with flattened seasonal cycles exhibit consistent patterns across all experiments, underestimating both the spring moisture accumulation and summer drawdown. EXP4a, which uses a loamy sand texture, shows greater seasonal responsiveness and more closely tracks ERA5-Land. The remaining EXP4 configurations (loam, with higher clay, silt) progressively dampen seasonal variability, reflecting the influence of soil moisture in winter texture on water retention and lower soil moisture in summerhydrologic dynamics.

470 3.4 EOF Analysis of Soil Moisture Variability

475

480

3.4.1 Explained Variance and Mode Contributions

This study applies EOF analysis to soil moisture anomalies from the CLM5 simulations (EXP1, EXP2, EXP3) and ERA5-Land data to investigate how soil parameterization influences soil moisture variability in the CONUS region. Figure 6-8 presents the percentage of variance explained by the first 10 EOF modes for each dataset, illustrating both individual and cumulative contributions. The EOF modes are ranked by variance percentage, with EOF-1 capturing the highest variance and representing the most significant spatial variability. Across all experiments, EOF-1 explains slightly more variance than EOF-2, suggesting limited separation between these modes and potential mode mixing. The explained variance gradually declines in subsequent modes, with EOF-10 contributing less than 2%, as summarized in Table 3. EOF-1 explains a similar percentage of variance in EXP1 (11.45%) and EXP2 (11.66%), indicating comparable spatial variability patterns. However, in EXP3, EOF-1 captures only 10.84% of the variance, with mode mixing shifting variance from EOF-1 to EOF-2 (Table 3, arrows). These differences highlight the impact of soil parameterization on representing dominant soil moisture variability. ERA5-Land, serving as a benchmark, exhibits a much stronger EOF-1 contribution (17.5%), emphasizing a more dominant leading mode in observed

data compared to modeled datasets. The cumulative explained variance (Figure 8, green line) further demonstrates the efficiency of the EOF modes in capturing soil moisture variability.

While the first five modes account for about 40% of the variance in ERA5-Land, modeled datasets require approximately six modes to reach the same threshold. This distribution suggests that simulations spread variance more evenly across modes, reflecting differences in spatial patterns between models and observations. To ensure comparability, adjustments aligned the EOF modes across datasets. For instance, shifts in EXP3 and ERA5-Land were necessary to match dominant spatial patterns, such as EOF-1 and EOF-2 swaps (marked in red and blue in indicated by arrows in Table 3). These adjustments highlight the sensitivity of EOF rankings to mode mixing and the challenges of directly comparing modeled and observed datasets. In addition, Appendix A (Figure A1) provides additional EOF analysis results for EXP4a-d, detailing variance explained across experiments. The findings reinforce the influence of soil parameterization on the spatial distribution of soil moisture and emphasize the need for improved alignment with observed patterns, as reflected in ERA5-Land.

Table 3. Percentage of variance explained (%Expl. Var.) by the first 10 EOF modes for EXP1, EXP2, and EXP3 model runs, and ERA5-Land benchmark data. Arrows and superscripts indicate EOF mode swaps for consistent comparisons across datasets (see Figure 9).

EOF Mode	EXP1 %Expl. Var.	EXP2 %Expl. Var.	EXP3 %Expl. Var.	ERA5-Land %Expl. Var.
EOF-1	11.45	11.66	$10.8410.84 \downarrow^2$	$17.5 17.5 \downarrow^2$
EOF-2	10.40	10.60	9.85 9.85 ↑¹	8.48 <u>8.48</u> ↓ ³
EOF-3	8.81	8.25	9.08	7.83 - 7.83 ↑¹
EOF-4	5.69	5.83	5.73	5.75
EOF-5	4.37	4.59	4.48	5.61
EOF-6	3.49	3.56	3.48	3.64
EOF-7	3.26	3.23	3.24	3.10
EOF-8	2.51	2.53	2.63	2.86
EOF-9	2.14	2.16	2.22	2.76
EOF-10	1.96	1.99	1.95	2.22
Total Cumm. %Expl. Var.	54.07	<u>54.4</u>	53.49	59.77

3.4.2 Spatial and Temporal Analysis of EOF Modes for Soil Moisture Variability

485

490

Spatial distribution of the first three EOF modes from soil moisture anomalies in CLM5 simulations (EXP1, EXP2, EXP3) and ERA5-Land (control). The correlation coefficients, ranging from -1 to +1, indicate the reference). The maps in Figure 9 show correlation coefficients between the PC time series of each EOF mode and the soil moisture anomaly time series at each grid point. These correlation maps indicate the spatial strength and direction of the relationship between EOF patterns and soil moisture anomalies (Figure 9) association between local anomalies and the broader temporal mode represented by the PC.

This representation facilitates interpretation by highlighting regions that co-vary in phase (positive correlation) or in anti-phase (negative correlation) with the dominant temporal pattern, thereby revealing the spatial structure of soil moisture variability

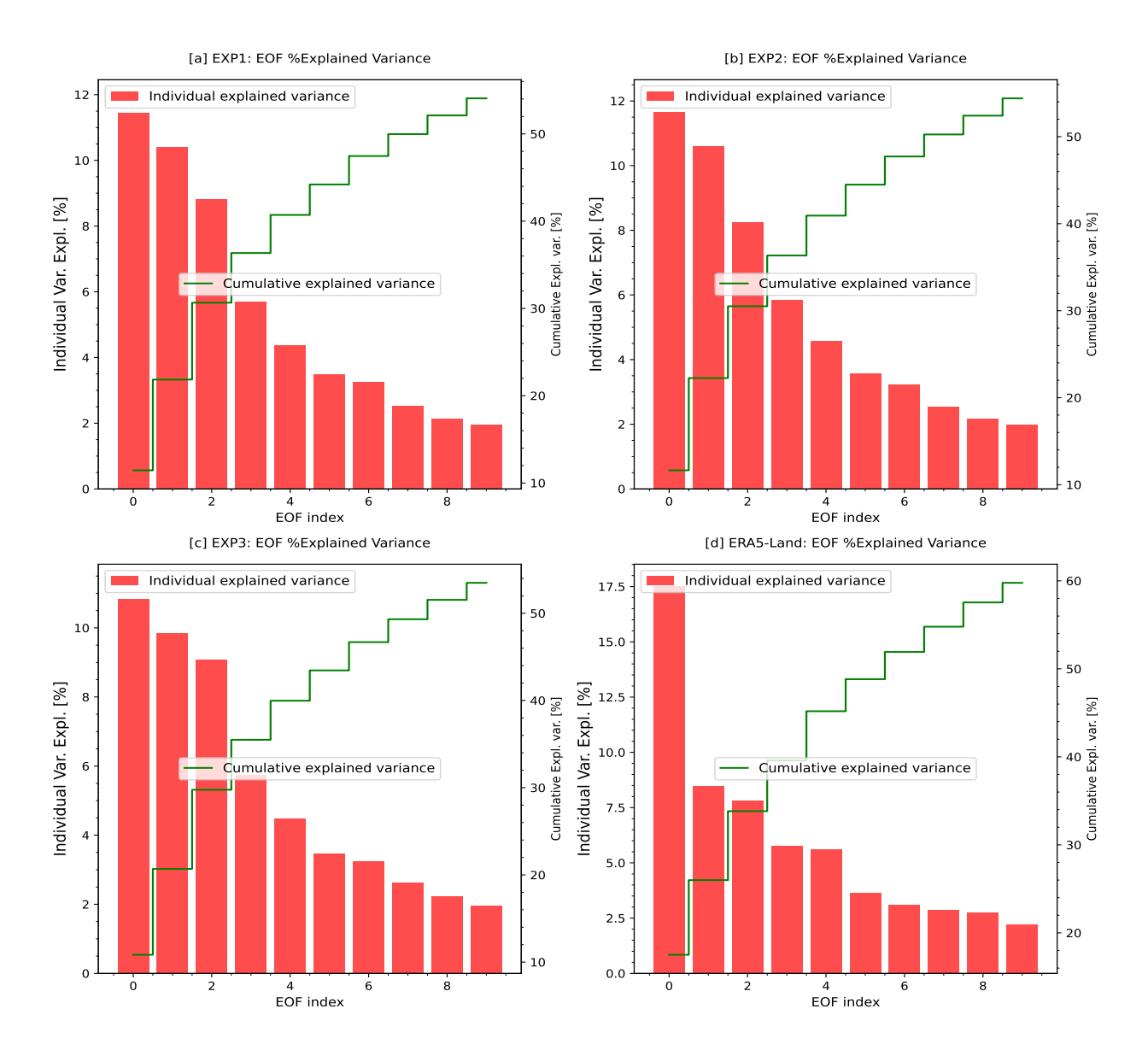


Figure 8. The variance explained by each separate and combined EOF in the CLM5 soil moisture experiment is depicted. Red bars represent the contribution of each EOF individually, while the green line shows the cumulative proportion for the initial 10 EOF modes.

linked to each EOF mode. EOF-1 patterns (Figures 9d, g, j) reveal strong positive correlations in central and southeastern ENA, highlighting a dominant mode of variability. Negative correlations are observed in WNA and CNA, indicating contrasting modes of soil moisture variability in the CONUS region. The variance explained by EOF-1 ranges from 9.85% (EXP3) to 11.66% (EXP2), with ERA5-Land explaining significantly more variance at 17.5%. These spatial patterns align with large-scale climatic influences such as precipitation gradients and geographic features. For example, Gaffin and Hotz (2000) noted

that the Appalachian Mountains exhibit strong precipitation gradients due to storm systems lifting moist southerly winds, enhancing soil moisture in ENA. The corresponding principal components (PC-1; Figure 10a) indicate temporal variability, with notable peaks during 2003 to 2004 and 1988 to 1999, corresponding to documented climatic events such as ENSO-driven precipitation anomalies (Ye et al., 2023; Gimeno et al., 2010). The close agreement of PC-1 across all experiments highlights the robustness of EOF-1 in representing dominant soil moisture variability, although slight differences suggest sensitivity to parameterizations.

510

520

525

530

535

EOF-2 (Figures 9e, h, k) exhibits a distinct dipole pattern, with positive correlations in the central Great Plains and negative correlations over ENA, reflecting a wide spread in soil moisture variability. This dipole nature, which explains 10.40% to 10.84% of the variance, is consistent with regional climatic processes such as precipitation and evapotranspiration dynamics influenced by terrain and hydrological conditions. For example, positive correlations in the central Great Plains may result from localized convective precipitation; however, isotope studies indicate that precipitation in this region is influenced by moisture transported from external sources, such as the Gulf of Mexico, rather than solely from local convection (Sanchez-Murillo et al., 2023). Negative correlations in ENA could reflect the influence of evapotranspiration or soil drainage patterns (Famiglietti, 2014). In particular, EXP3 shows a stronger positive correlation in the desert southwest, indicating a greater sensitivity to soil parameters in arid regions, which can alter soil water retention and infiltration rates. Furthermore, EOF-3 (Figures 9f, i, 1) highlights localized variability, with positive correlations in the Pacific Northwest and negative correlations over Texas in CNA. This mode explains less variance than EOF-1 and EOF-2, ranging from 8.25% (EXP2) to 9.85% (EXP3), but captures important regional processes. The Pacific Northwest patterns may be influenced by orographic precipitation, while negative correlations in Texas could reflect drought conditions dominated by soil type and fine texture which have a high potential for water retention (Haverkamp et al., 2005) and fine-texture which have a high potential for water retention. Although the spatial patterns of EOF-3 are broadly similar between experiments, slight shifts in correlation intensity and location suggest localized impacts of soil parameterizations. The PCs (Figure 10c) show weaker temporal variability, with occasional peaks corresponding to distinct climate events, which emphasizes the regional specificity of EOF-3. The appendix includes Figures A2 and A3, which offer additional results highlighting the spatial and temporal variability of EXP4a-d EOF across experiments, further supporting the findings discussed. Lastly, the results emphasize the significant role that soil parameterizations play in soil moisture variability within the CLM5 model. Differences in the spatial and temporal patterns of EOFs indicate the model's sensitivity to these parameterizations, especially in areas with intricate terrain or significant climate variability. The alignment of EOF-1 with ERA5-Land underscores the robustness of the model's primary modes, while discrepancies in EOF-2 and EOF-3 highlight regions where model refinements could enhance localized soil moisture predictions. This study stresses the importance of improving soil parameterizations to increase the precision of hydrological simulations and effectively capture the interaction between soil moisture and climatic elements.

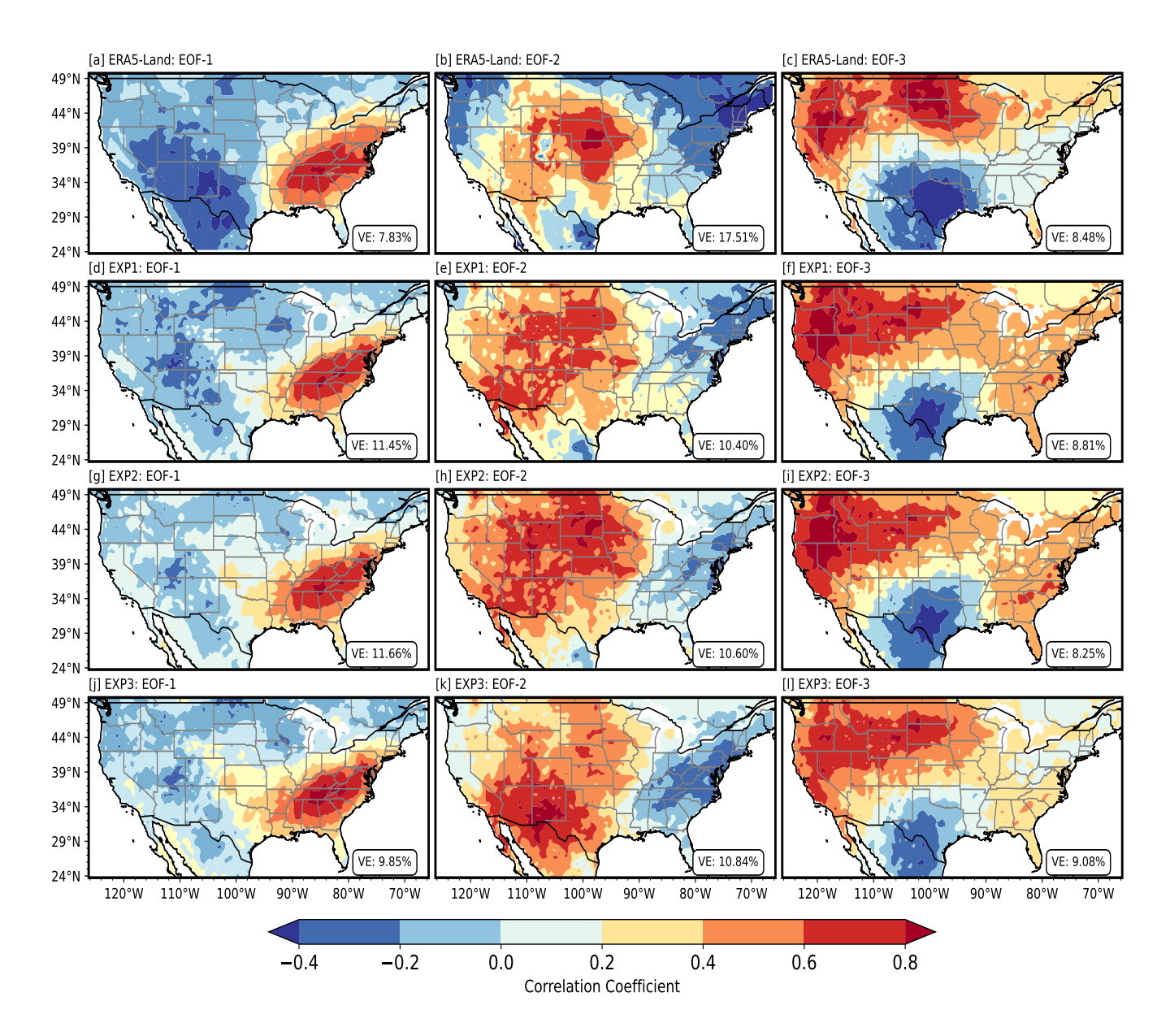


Figure 9. Spatial patterns correlation maps of the first three Empirical Orthogonal Functions (EOFs) of soil moisture anomalies for the continental United States CONUS, derived from ERA5-Land reanalysis data and three different experimental model runs CLM5 experiments (EXP1, EXP2, EXP3). Panels (a) to (c) represent EOF-1, EOF-2, and EOF-3 from the ERA5-Landdataset, respectively. Panels (d-f), (g-i), and (j-l) show corresponding modes from EXP1, EXP2, and EXP3. The color shading indicates represents the correlation coefficient ; between the PC time series of each EOF mode and the soil moisture anomaly time series at each grid point. Positive values indicate in-phase variability with blue representing the PC (regions that co-vary with the dominant mode), while negative values indicate anti-phase behavior. These maps illustrate the spatial coherence and red representing positive correlations phase relationships of soil moisture variability associated with each mode.

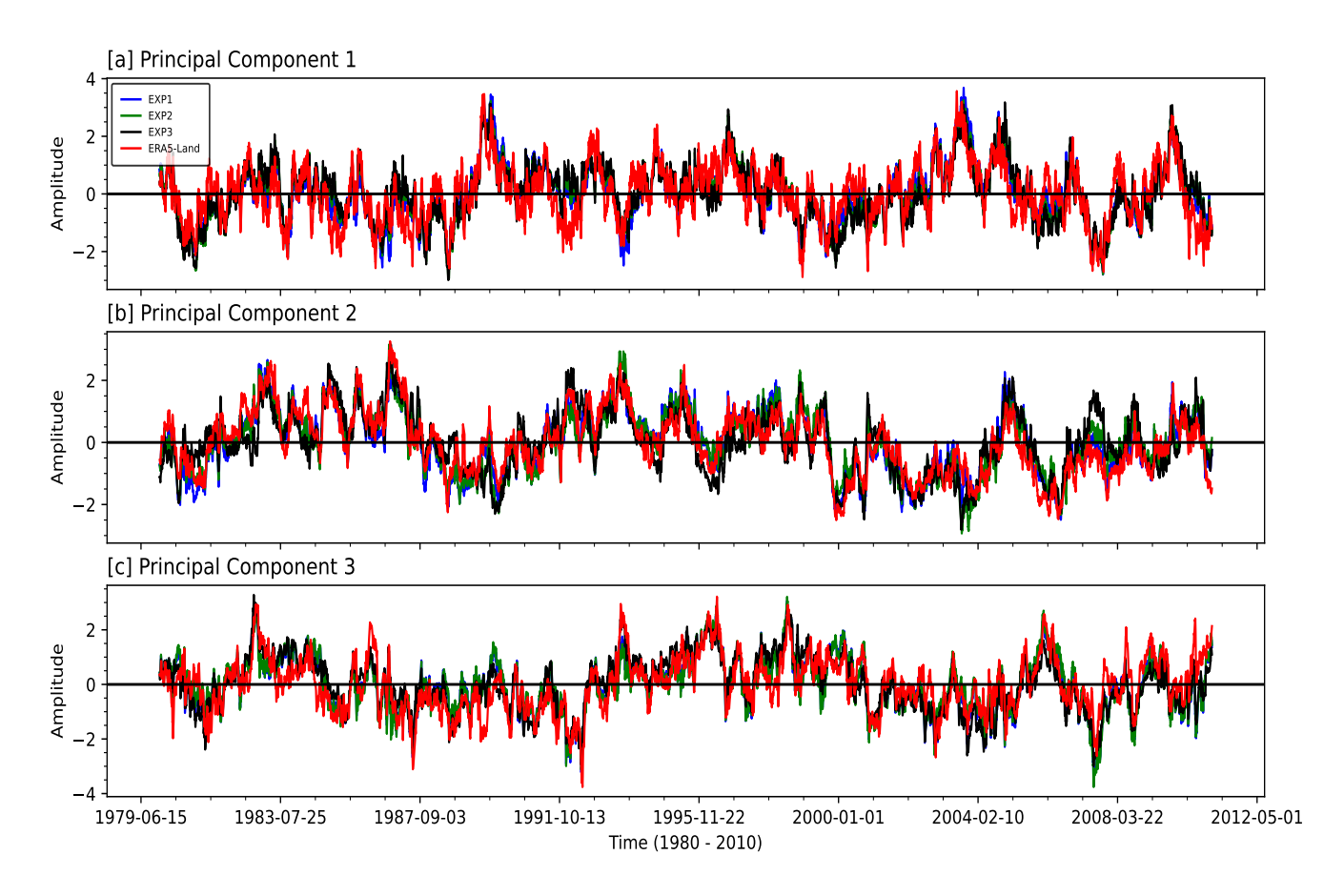


Figure 10. Temporal Variability (PC) of corresponding EOF over time (1980-2010) displaying the amplitude of the first four PCs: EXP1 (blue), EXP2 (green), and EXP3 (orange) derived from the soil moisture decomposition respective of their simulation experiments.

3.4.3 EOF Modes: Euclidean Distance Analysis

540

The Euclidean distance between the spatial patterns of EOF modes derived from soil moisture anomalies in CLM5 SP-MIP model experiments (EXP1, EXP2, and EXP3) and the corresponding EOF modes from the ERA5-Land reanalysis (Figure 11). The Euclidean distance quantifies the dissimilarity between the spatial modes, with smaller values indicating closer agreement with the ERA5-Land benchmark. Regions with hatched lines represent areas where the Euclidean distance falls below a threshold of 5, suggesting a strong alignment between the model-derived EOFs and the observed EOFs in these locations. EOF-1 exhibits the most consistent alignment across experiments, particularly in the western and northwestern portions of the CONUS region (WNA). The hatched areas in these regions indicate that the spatial variability of soil moisture in these areas is well-represented by the model, reflecting accurate capture of large-scale hydrological processes influenced by precipitation gradients and topographic features (Gaffin and Hotz, 2000; Famiglietti, 2014). In contrast, the central Great Plains consistently shows larger Euclidean distances for all three EOF modes across experiments, suggesting significant discrepancies between

the modeled and observed soil moisture patterns in this region. This discrepancy may be attributed to limitations in soil parameterizations or the complexity of hydrological and climatic processes, such as precipitation variability and soil moisture precipitation feedbacks, as highlighted by Koster et al. (2004) and Welty and Zeng (2018). Compared to ERA5-Land, EXP1 shows a better agreement with ERA5-Land in the WNA region for EOF-1, while the performance in other regions remains mixed across the experiments. EOF-2 and EOF-3 exhibit increased variability in Euclidean distances, with fewer hatched areas, indicating challenges in capturing smaller-scale processes and dipole patterns present in these modes (Hannachi et al., 2007; Monahan et al., 2009). These findings underscore the model's sensitivity to parameterizations and highlight the need for targeted improvements in the central Great Plains and other regions with persistent discrepancies. By refining soil parameter settings and incorporating additional observational constraints, future experiments could achieve better alignment with ERA5-Land, thereby enhancing the accuracy of regional soil moisture simulations (Lawrence et al., 2019; Tuttle and Salvucci, 2016).

550

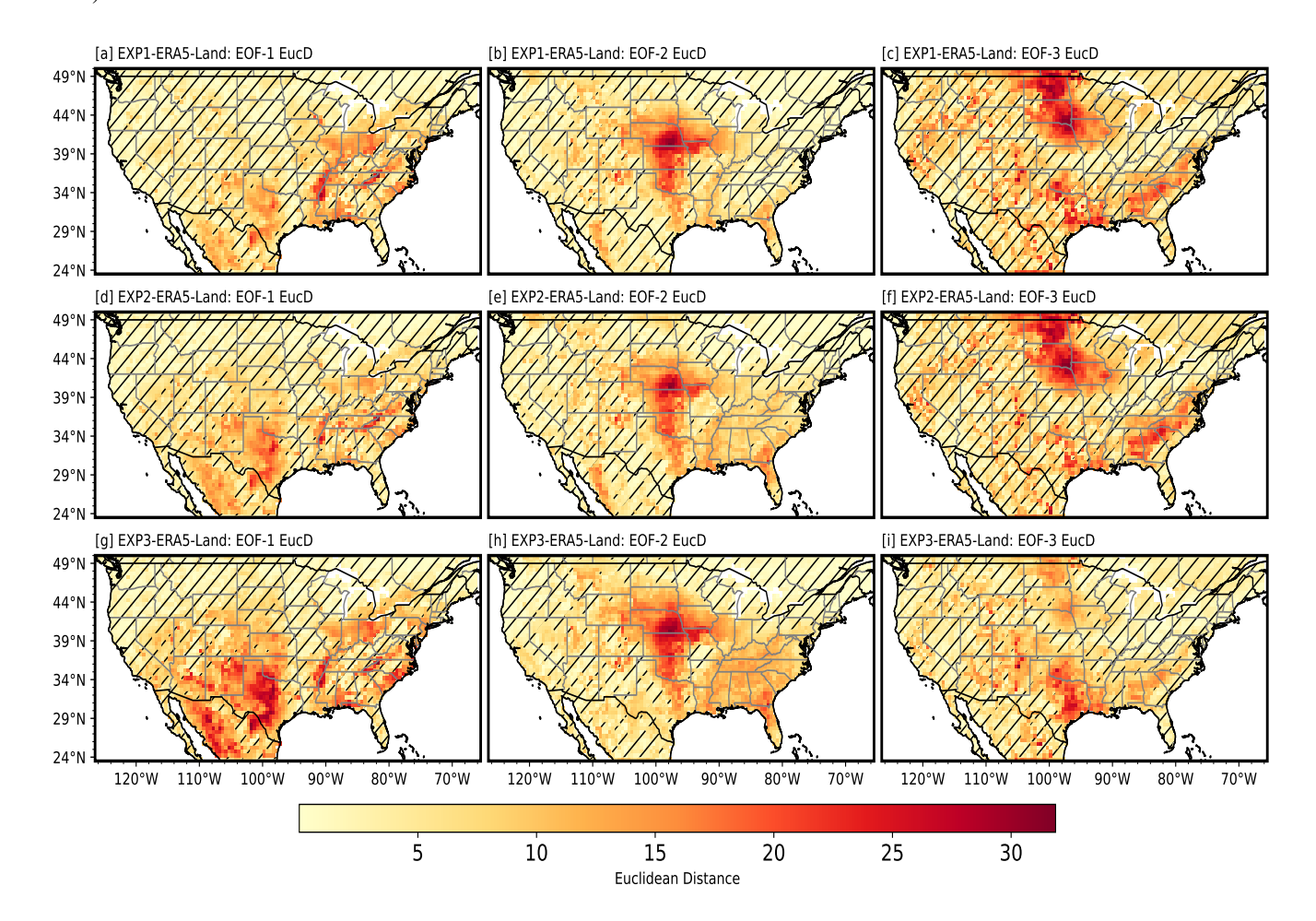


Figure 11. Euclidean distance between EOF modes from SP-MIP experiments (EXP1, EXP2, EXP3) and ERA5-Land. Hatched areas indicate regions where the distance is below the threshold of 5, showing closer agreement with ERA5-Land.

3.4.4 EOF Modes: Taylor Diagram Analysis

560

565

570

575

TDs (Figure 12) provide a comprehensive statistical summary of how well EOF patterns from different experiments match those of ERA5-Land by depicting three key statistics: the standard deviation (dotted lines), the correlation coefficient, and the centered root mean square error (RMSE). Each marker's position on the plot indicates how accurately the soil moisture EOF mode pattern aligns with the ERA5-Land EOF mode. For EOF-1 (Figure 12a), the standard deviations of the EOF modes for all model experiments are relatively close to the reference EOF mode, ranging between 4.0 and 6.5, which suggests a good match in terms of variability. The pattern correlations range between 0.6 and 0.95, with EXP4d demonstrating the highest pattern correlation. This indicates that the spatial pattern of EXP4d aligns more closely with the ERA5-Land EOF mode. In EOF-2 (Figure 12b), the standard deviations remain consistent with the reference EOF mode, while the pattern correlations cluster between 0.4 and 0.7. This highlights a moderate similarity in the spatial patterns of EOF across the experiments and in the reference EOF mode for the second mode of variability. For EOF-3 (Figure 12c), the EOF modes generally exhibit a pattern correlation of around 0.8 and a standard deviation of approximately 5.0. However, the EXP4d EOF deviates, centered around a lower standard deviation of 3.5. These variations emphasize the influence of soil parameter settings in the simulations of the CLM5 model, illustrating how adjustments in these settings affect the alignment of the EOF mode patterns with the ERA5-Land reference EOF mode.

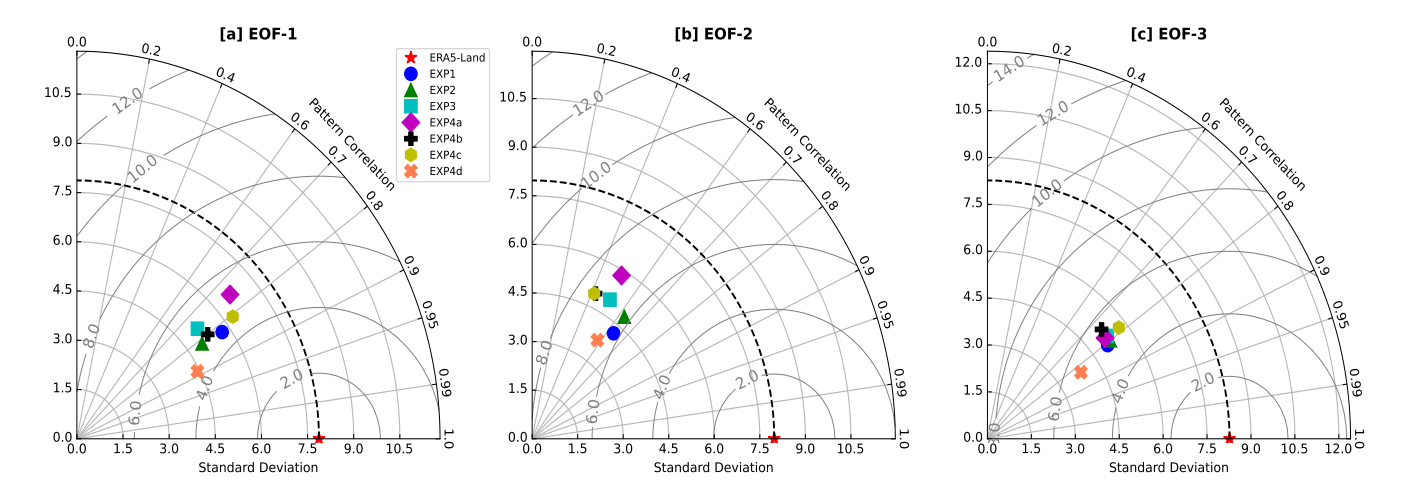


Figure 12. Taylor Diagrams (TDs) for the leading three EOFs from multiple experiments (EXP1, EXP2, EXP3, EXP4a, EXP4b, EXP4c, EXP4d) and ERA5-Land. The diagrams summarize standard deviation, correlation coefficient, and RMSE, with marker placement indicating the alignment of modeled EOF modes with ERA5-Land.

4 Conclusion and Recommendations

This study investigates the influence of soil parameterizations on soil moisture simulations in the CLM5 across the CONUS for the period 1980 to 2010 using EOF analysis. The analysis compared the CLM5 outputs with the ERA5-Land reanalysis data to

identify spatial and temporal variability in soil moisture patterns arising from differences in soil parameter configurations. The results highlighted that EXP3, which used the default CLM5 soil parameters, consistently simulated higher soil moisture levels than other experiments. This finding underscores the model's sensitivity to variations in soil hydraulic properties, such as saturated hydraulic conductivity, soil water retention characteristics, and porosity. Seasonal soil moisture dynamics showed broad consistency across experiments, peaking in winter due to reduced evapotranspiration, and declining in summer when higher temperatures intensified soil drying. However, distinct differences emerged in the magnitude and phase of seasonal cycles, revealing how variations in soil properties can influence processes such as water retention, drainage, and evapotranspiration fluxes. These insights align with previous research, which demonstrated that soil moisture significantly affects hydrological processes and land-atmosphere interactions, particularly through feedback mechanisms that vary regionally across the United States ((Tuttle and Salvucci, 2016; Koster et al., 2004). Furthermore, the amplified sensitivity observed in the arid and semi-arid regions of the CONUS suggests that these areas may be particularly vulnerable to uncertainties in soil parameterization.

EOF analysis This study directly addressed two key research questions: (1) how soil hydraulic parameters influence large-scale spatial soil moisture patterns, and (2) how these parameters affect temporal dynamics during climate extremes. Regarding the first question, EOF analysis revealed that changes in soil hydraulic properties significantly altered the spatial distribution of dominant EOF modes, particularly in regions like the Great Plains and ENA, indicating that parameterizations strongly shape modeled soil moisture gradients. For the second question, principal component time series linked to major EOFs captured interannual anomalies and periods of extreme wetness or dryness that aligned with known climate events, such as ENSO phases. Variations in the amplitude and persistence of these temporal patterns across experiments underscored the role of soil parameters in modulating the hydrologic response to climate variability. These findings affirm that parameter choice not only controls spatial representation but also governs the sensitivity of soil moisture to climatic extremes, highlighting the dual spatial-temporal impact of soil parameterization in land surface modeling.

EOF analysis further revealed that the first few modes accounted for the majority of the variance in soil moisture between experiments, and the EOF-1 mode, decomposed from soil moisture consistently explained the largest proportion. The spatial patterns of the first three EOF modes exhibited similar broad-scale features among the experiments, such as dominant moisture gradients across climatic zones. However, notable differences in explained variance and spatial correlations pointed to the influence of soil parameters on the physical processes driving regional moisture variability. Compared with ERA5-Land data using Euclidean distances and Taylor diagrams, the CLM5 output aligned more closely with observations in WNA, reflecting better model performance in capturing the dynamics of mountainous and arid regions. In contrast, persistent discrepancies in the central Great Plains revealed challenges in representing complex interactions between soil hydraulic properties, precipitation variability, and surface-atmosphere feedbacks. These discrepancies are particularly concerning given the region's susceptibility to extreme hydrological events, including droughts and floods (Koster et al., 2004; Ye et al., 2023). The Great Plains is characterized by a highly variable continental climate, with strong seasonal and interannual fluctuations in precipitation and temperature, leading to frequent shifts between wet and dry extremes (Basara and Christian, 2018; McDonough et al., 2020). This climatic variability makes the region hydrologically complex, requiring accurate representation of soil moisture dynamics for land surface hydrology modeling. Errors in soil moisture estimation can propagate into predictions of crop productivity,

water resource availability, and flood risk. The findings suggest that refining soil hydraulic parameterizations, such as incorporating high-resolution soil texture data and accounting for heterogeneity, can significantly improve the predictive capacity of CLM5 and other land surface models LSMs for climate studies, ecosystem assessments, and resource management. While our comparative framework assessed the aggregate effects of parameter set differences, we did not perform a formal sensitivity analysis to isolate the influence of individual soil hydraulic properties (e.g., saturated hydraulic conductivity, porosity, van Genuchten parameters), which remains an important area for future investigation.

While ERA5-Land was used as the reference dataset in this study, we emphasize that our objective was not to perform a traditional comparison of CLM5 soil moisture outputs, but to evaluate the intra-model sensitivity of spatial and temporal variability to different soil hydraulic parameterizations. ERA5-Land served as a physically consistent and spatially continuous benchmark to assess whether CLM5's simulated patterns of variability were realistic and coherent. Its compatibility with the model's spatial and temporal resolution, broad spatial coverage, and representation of seasonal and interannual dynamics made it appropriate for the pattern-oriented objectives of this work. We acknowledge the limitations of ERA5-Land, particularly its lack of direct in-situ soil moisture assimilation and potential biases in humid regions (Muñoz-Sabater et al., 2021; Wu et al., 2021; Zhang et , but used it primarily to benchmark the structure of variability, not the absolute magnitude of soil moisture. Future research will build upon this diagnostic framework by incorporating observational datasets such as SMAP, GLEAM (Martens et al., 2017), SMERGE (Tobin et al., 2019), or MERRA-2 (Reichle et al., 2017), which will enable a more comprehensive comparison and facilitate targeted calibration of model parameters. For the present study, however, ERA5-Land provided a robust and consistent backdrop for assessing how parameter choices influence modeled variability patterns across diverse hydroclimatic regions.

To address these challenges and improve the accuracy of soil moisture simulation in CLM5, several strategies are recommended. Refinement of soil moisture variability representation using advanced PTFs or machine learning-based approaches can address uncertainties in soil hydraulic parameters, especially in hydrologically complex regions such as the Great Plains. Expanding the use of high-resolution datasets from satellite missions such as the Soil Moisture Active Passive (SMAP) SMAP mission and in situ soil moisture networks will provide robust benchmarks for calibration and validation comparison, reducing biases in model outputs (Famiglietti, 2014). Conducting region-specific calibration of soil parameters and comparative multimodel analyses will help address inter-model intra-model variability and optimize simulations for diverse climatic zones. Linking soil moisture variability to dynamic vegetation feedbacks can improve the representation of evapotranspiration processes, as vegetation significantly influences soil moisture and water exchange dynamics (Oleson et al., 2010; Ye et al., 2023). Establishing stronger connections between soil moisture variability and large-scale climatic drivers such as the ENSO can enhance seasonal forecasts and long-term predictive capabilities (Gimeno et al., 2010; Tuttle and Salvucci, 2016). Understanding these links will facilitate better integration of climatic variability into land surface modeling frameworks.

Importantly, these findings also open the door to future efforts that incorporate dynamic soil properties into LSMs. Much of this work demonstrates the dynamism of soil properties, and while this study advances modeling by revealing the importance of their inclusion, the next crucial step will be developing approaches that allow these properties to be dynamic within LSMs. This paper serves as a foundational step toward that goal, paving the way for more complex and integrated modeling frameworks that better capture soil-hydrology-climate interactions. These recommendations aim to address existing challenges in

soil moisture modeling and improve the predictive capabilities of land surface models LSMs such as CLM5. Advancing soil hydraulic parameterization and leveraging state-of-the-art observational datasets will enable models to more accurately capture large-scale hydrological dynamics and localized soil-climate interactions. This, in turn, will support improved water resource management, agricultural planning, and climate adaptation strategies, ultimately contributing to the larger goals of sustainable development and climate resilience.

650

655

Code and data availability. All datasets used in this study are publicly for download at Zenodo https://doi.org/10.5281/zenodo.15078448 (Silwimba, 2025b). This includes files on soil parameters and soil texture for EXP1, EXP2, and EXP4a–d. Additionally, the ERA5-Land can be freely accessed at https://doi.org/10.24381/cds.e9c9c792 (Muñoz-Sabater et al., 2021). The code used to process the data, perform the EOF analyses, and generate the results is available on Zenodo at https://doi.org/10.5281/zenodo.14888812 (Silwimba, 2025a). The Zenodo repository provides comprehensive documentation and instructions for reproducing the analysis, and any future updates or additional scripts will be hosted there. For any difficulties in accessing these data or code, or for requests for further information, please contact the corresponding author.

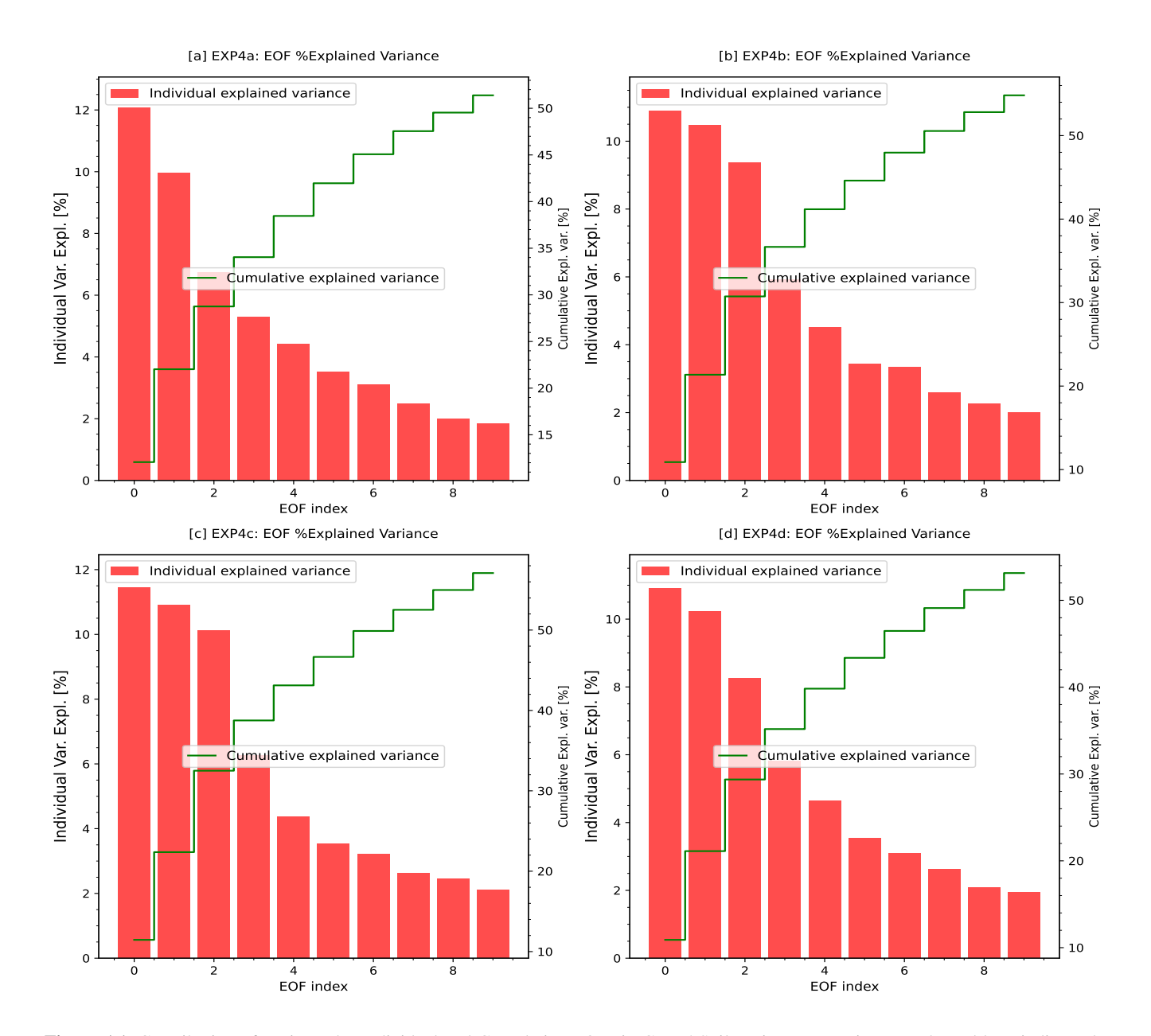


Figure A1. Contribution of Variance by Individual and Cumulative EOFs in CLM5 Soil Moisture Experiments. The red bars indicate the portion of variance each separate EOF mode accounts for, whereas the green line depicts the cumulative percentage of variance explained by the first ten EOF modes. These plots reveal the significant impact of the early EOF modes in accounting for variance. Panels (a) to (d) relate to different experimental configurations or scenarios, offering a comparative assessment of EOF variance contributions.

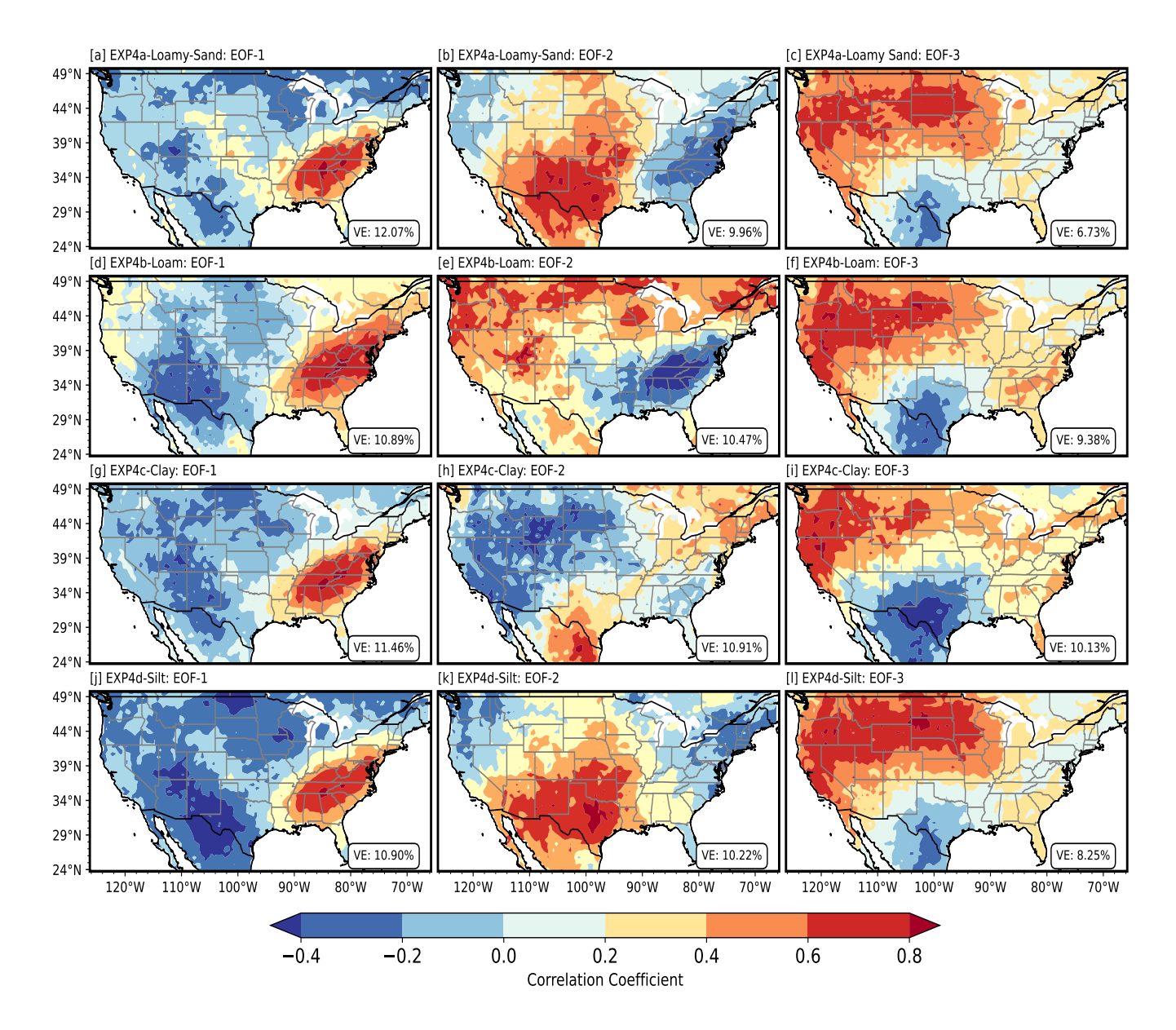


Figure A2. The initial three EOF modes' spatial Spatial correlation patterns resulting from maps of the first three Empirical Orthogonal Functions (EOFs) of soil moisture decomposition anomalies across the CONUS region are depicted domain for the EXP4 simulations. Panels (a, b, c) are for correspond to Experiment 4a (Loamy Sand), (d, e, f) for to Experiment 4b (Loam), (g, h, i) for to Experiment 4c (Clay), and (j, k, l) for to Experiment 4d (Silt). Each panel displays the first (set shows EOF-1), second (EOF-2), and third (EOF-3) EOF modes, respectively. Within each panel, The color shading represents the variance explained correlation coefficient between the principal component (VEPC) by the time series of each EOF modes is noted, with EOF-1 consistently exhibiting mode and the highest VE across all soil typesmoisture anomaly time series at each grid point. The color gradient Positive values (blue to red) indicates indicate locations that vary in phase with the correlation coefficient mode's temporal evolution, with red signifying a strong positive correlation and blue a strong while negative onevalues (blue) indicate anti-phase behavior. The variance explained (VE) by each mode is noted in each panel. These patterns showcase correlation maps illustrate how the spatial structure of soil moisture decomposition's spatial variability is shaped influenced by distinct soil textures hydraulic properties associated with each texture 4ass.

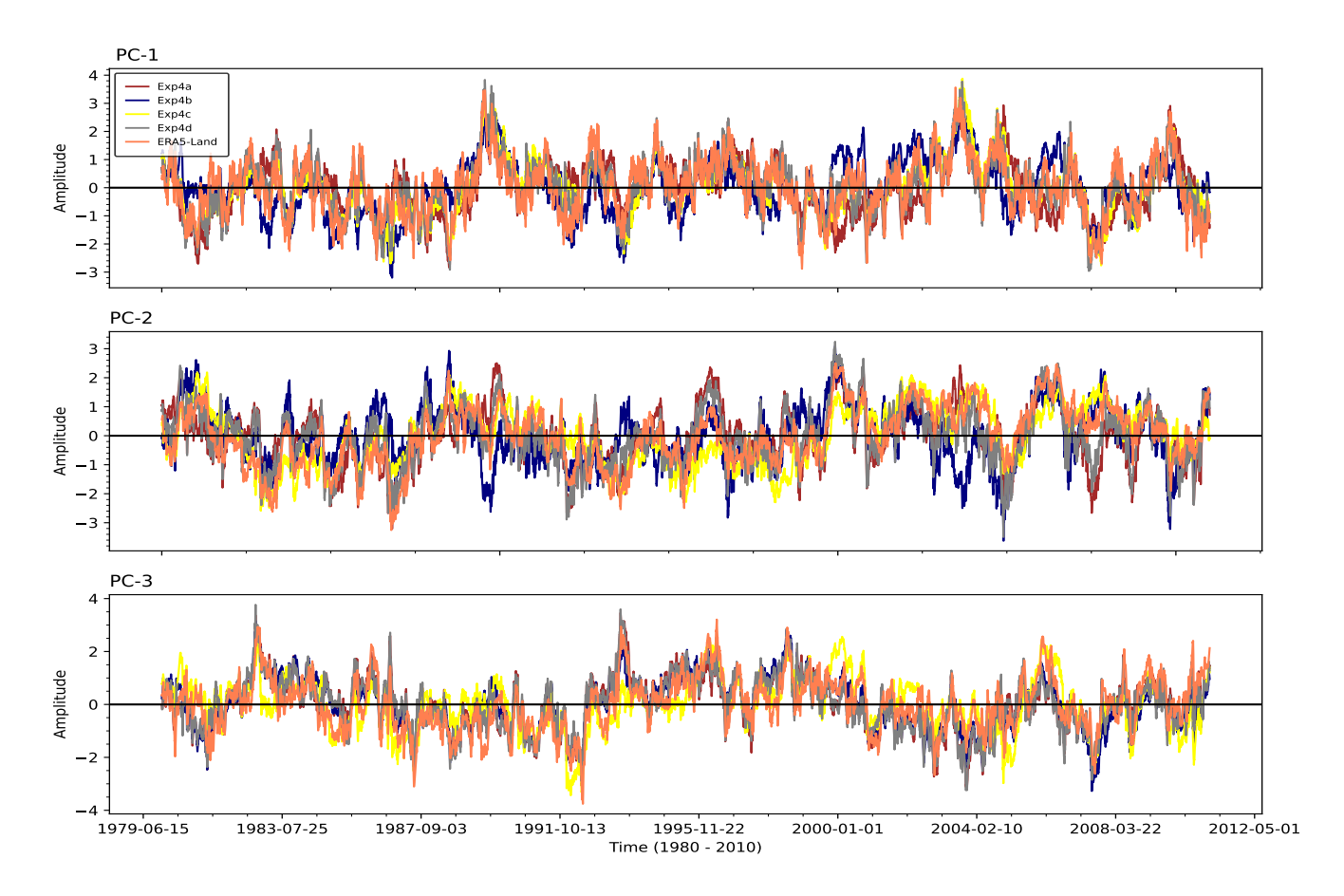


Figure A3. Temporal variability of principal components (PCs) derived from the EOF analysis. The plots display the amplitude of the first three principal components: PC-1, PC-2, and PC-3. Each line corresponds to one of the four experimental setups (EXP4a, EXP4b, EXP4c, and EXP4d) or the ERA5-Land reanalysis. PC-1 (top panel) captures the dominant mode of variability, while PC-2 (middle panel) and PC-3 (bottom panel) represent the secondary and tertiary modes, respectively. The x-axis shows the time period (1979–2012), and the y-axis indicates the standardized amplitude. These plots highlight the temporal dynamics of soil moisture variability as captured by different experimental configurations, providing insights into their agreement and divergence relative to the ERA5-Land reference data.

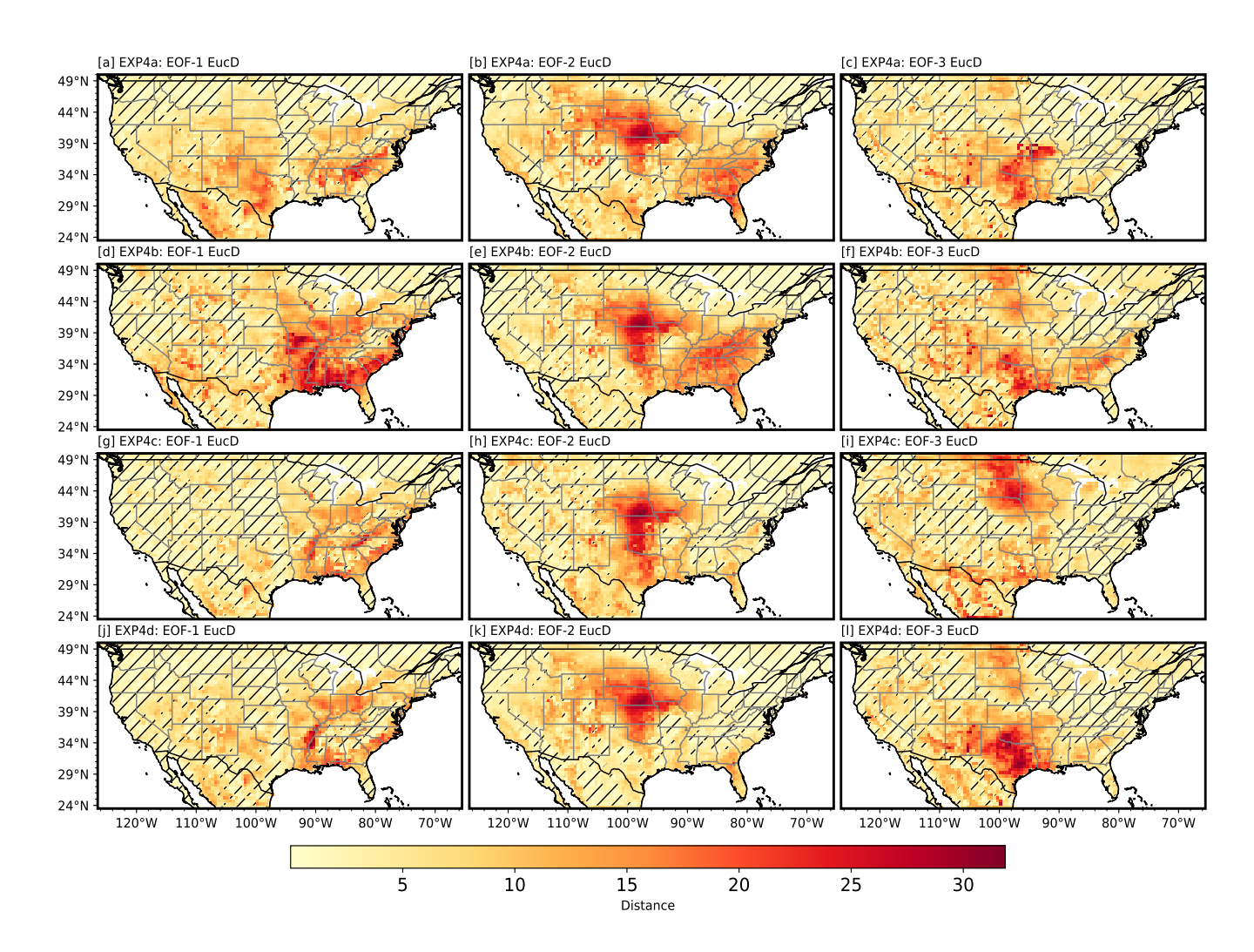


Figure A4. The Euclidean distance between EOF modes from SP-MIP experiments (EXP4a, EXP4b, EXP4c, EXP4d) and ERA5-Land is depicted. Panels (a–c) illustrate results for Experiment 4a (Loamy Sand), while panels (d–f), (g–i), and (j–l) pertain to Experiments 4b (Loam), 4c (Clay), and 4d (Silt), respectively. Each column showcases one of the first three EOF modes: EOF-1, EOF-2, and EOF-3. The color bar represents the Euclidean distance, where lower values (yellow) reflect stronger alignment with ERA5-Land, whereas higher values (red) denote more significant discrepancies. Regions with hatched patterns signify distances less than 5, emphasizing areas where the experiments closely align with the ERA5-Land data. These observations reveal the spatial variability in model performance across different soil hydraulic parameter settings and EOF modes.

Competing interests. The authors declare that they have no conflicts of interest.

Acknowledgements. We acknowledge funding support from the National Science Foundation Frontiers Research in Earth Science program (HA & DRH - 2121760; PLS - 2121694; SAB - 2121639; LL - 2121621; AF - 2121595). Additional support was provided by the Signals in the Soil (SitS) grant from the USDA National Institute of Food and Agriculture (HA & DRH - no. 2021-67019-34341; SAB - no. 2021-67019-34338; ANF - no. 2021-67019-34340) and by the National Science Foundation under Grant Nos. 2034232 (PLS) and 2034214 (LL). We also acknowledge support from the National Science Foundation EAR program under Grant Nos. 2034232 and 2121694.

We thank Jesse Nippert for valuable feedback, which helped improve this work.

665

Any opinions, findings, and conclusions or recommendations expressed in this material are those of the authors and do not necessarily reflect the views of the National Science Foundation.

670 References

- Basara, J. B. and Christian, J. I.: Seasonal and interannual variability of land–atmosphere coupling across the southern Great Plains of North America using the North American regional reanalysis, International Journal of Climatology, 38, 964–978, 2018.
- Bauer-Marschallinger, B., Dorigo, W. A., Wagner, W., and Van Dijk, A. I.: How oceanic oscillation drives soil moisture variations over mainland Australia: An analysis of 32 years of satellite observations, Journal of Climate, 26, 10159–10173, 2013.
- 675 Berg, A. and Sheffield, J.: Soil moisture–evapotranspiration coupling in CMIP5 models: Relationship with simulated climate and projections, Journal of Climate, 31, 4865–4878, 2018.
 - Björnsson, H. and Venegas, S.: A manual for EOF and SVD analyses of climatic data, CCGCR Report, 97, 112-134, 1997.
 - Brimelow, J. C., Hanesiak, J. M., and Raddatz, R.: Validation of soil moisture simulations from the PAMII model, and an assessment of their sensitivity to uncertainties in soil hydraulic parameters, Agricultural and Forest Meteorology, 150, 100–114, 2010.
- 680 Brocca, L., Ciabatta, L., Massari, C., Camici, S., and Tarpanelli, A.: Soil moisture for hydrological applications: Open questions and new opportunities, Water, 9, 140, 2017.
 - Caplan, J. S., Giménez, D., Hirmas, D. R., Brunsell, N. A., Blair, J. M., and Knapp, A. K.: Decadal-scale shifts in soil hydraulic properties as induced by altered precipitation, Science advances, 5, eaau6635, 2019.
 - Chatterjee, S., Desai, A. R., Zhu, J., Townsend, P. A., and Huang, J.: Soil moisture as an essential component for delineating and forecasting agricultural rather than meteorological drought, Remote Sensing of Environment, 269, 112 833, 2022.
 - Clapp, R. B. and Hornberger, G. M.: Empirical equations for some soil hydraulic properties, Water resources research, 14, 601–604, 1978.
 - Cosby, B., Hornberger, G., Clapp, R., and Ginn, T.: A statistical exploration of the relationships of soil moisture characteristics to the physical properties of soils, Water resources research, 20, 682–690, 1984.
- da Silva, L. d. C. M., Amorim, R. S. S., Fernandes Filho, E. I., Bocuti, E. D., and da Silva, D. D.: Pedotransfer functions and machine learning: Advancements and challenges in tropical soils, Geoderma Regional, 35, e00720, 2023.
 - Dagon, K., Sanderson, B. M., Fisher, R. A., and Lawrence, D. M.: A machine learning approach to emulation and biophysical parameter estimation with the Community Land Model, version 5, Advances in Statistical Climatology, Meteorology and Oceanography, 6, 223–244, 2020.
- Dai, Y., Xin, Q., Wei, N., Zhang, Y., Shangguan, W., Yuan, H., Zhang, S., Liu, S., and Lu, X.: A global high-resolution data set of soil hydraulic and thermal properties for land surface modeling, Journal of Advances in Modeling Earth Systems, 11, 2996–3023, 2019.
 - Dawson, A.: eofs: A library for EOF analysis of meteorological, oceanographic, and climate data, Journal of Open Research Software, 4, 2016.
 - De Lannoy, G. J., Koster, R. D., Reichle, R. H., Mahanama, S. P., and Liu, Q.: An updated treatment of soil texture and associated hydraulic properties in a global land modeling system, Journal of Advances in Modeling Earth Systems, 6, 957–979, 2014.
- De Rosnay, P., Drusch, M., Vasiljevic, D., Balsamo, G., Albergel, C., and Isaksen, L.: A simplified extended Kalman filter for the global operational soil moisture analysis at ECMWF, Quarterly Journal of the Royal Meteorological Society, 139, 1199–1213, 2013.
 - Elmore, K. L. and Richman, M. B.: Euclidean distance as a similarity metric for principal component analysis, Monthly weather review, 129, 540–549, 2001.
 - Famiglietti, J. S.: The global groundwater crisis, Nature climate change, 4, 945–948, 2014.
- 705 Feki, M., Ravazzani, G., Ceppi, A., and Mancini, M.: Influence of soil hydraulic variability on soil moisture simulations and irrigation scheduling in a maize field, Agricultural water management, 202, 183–194, 2018.

- Fu, X., Jiang, X., Yu, Z., Ding, Y., Lü, H., and Zheng, D.: Understanding the key factors that influence soil moisture estimation using the unscented weighted ensemble Kalman filter, Agricultural and Forest Meteorology, 313, 108 745, 2022.
- Fu, X., Lyu, H., Yu, Z., Jiang, X., Ding, Y., Zheng, D., Huang, J., and Fang, H.: Effects of soil hydraulic properties on soil moisture estimation,

 Journal of Meteorological Research, 37, 58–74, 2023.
 - Gaffin, D. M. and Hotz, D. G.: A precipitation and flood climatology with synoptic features of heavy rainfall across the southern Appalachian Mountains, National Weather Digest, 24, 3–16, 2000.
 - Gimeno, L., Drumond, A., Nieto, R., Trigo, R. M., and Stohl, A.: On the origin of continental precipitation, Geophysical Research Letters, 37, 2010.
- 715 Giorgi, F. and Francisco, R.: Evaluating uncertainties in the prediction of regional climate change, Geophysical Research Letters, 27, 1295–1298, 2000.
 - Godoy, V. A., Zuquette, L. V., and Gómez-Hernández, J. J.: Scale effect on hydraulic conductivity and solute transport: Small and large-scale laboratory experiments and field experiments, Engineering geology, 243, 196–205, 2018.
- Guimberteau, M., Ciais, P., Ducharne, A., Boisier, J. P., Dutra Aguiar, A. P., Biemans, H., De Deurwaerder, H., Galbraith, D., Kruijt, B.,
 Langerwisch, F., et al.: Impacts of future deforestation and climate change on the hydrology of the Amazon Basin: a multi-model analysis
 with a new set of land-cover change scenarios. Hydrology and Earth System Sciences, 21, 1455–1475, 2017.
 - Gundmundsson, L. and Cuntz, M.: Soil Parameter Model Intercomparison Project (SP-MIP): Assessing the influence of soil parameters on the variability of Land Surface Models, 2017.
- Hagemann, S., Chen, C., Clark, D. B., Folwell, S., Gosling, S. N., Haddeland, I., Hanasaki, N., Heinke, J., Ludwig, F., Voss, F., et al.: Climate change impact on available water resources obtained using multiple global climate and hydrology models, Earth System Dynamics, 4, 129–144, 2013.
 - Hannachi, A., Jolliffe, I. T., and Stephenson, D. B.: Empirical orthogonal functions and related techniques in atmospheric science: A review, International Journal of Climatology: A Journal of the Royal Meteorological Society, 27, 1119–1152, 2007.
 - Hauser, E., Sullivan, P. L., Flores, A. N., Hirmas, D., and Billings, S. A.: Global-Scale Shifts in Rooting Depths Due To Anthropocene Land Cover Changes Pose Unexamined Consequences for Critical Zone Functioning, Earth's Future, 10, e2022EF002 897, 2022.
 - Haverkamp, R., Leij, F. J., Fuentes, C., Sciortino, A., and Ross, P.: Soil water retention: I. Introduction of a shape index, Soil science society of America journal, 69, 1881–1890, 2005.
 - Hengl, T., De Jesus, J. M., MacMillan, R. A., Batjes, N. H., Heuvelink, G. B., Ribeiro, E., Samuel-Rosa, A., Kempen, B., Leenaars, J. G., Walsh, M. G., et al.: SoilGrids1km—global soil information based on automated mapping, PloS one, 9, e105 992, 2014.
- Hirmas, D. R., Giménez, D., Nemes, A., Kerry, R., Brunsell, N. A., and Wilson, C. J.: Climate-induced changes in continental-scale soil macroporosity may intensify water cycle, Nature, 561, 100–103, 2018.
 - Jawson, S. D. and Niemann, J. D.: Spatial patterns from EOF analysis of soil moisture at a large scale and their dependence on soil, land-use, and topographic properties, Advances in Water Resources, 30, 366–381, 2007.
- Ji, P., Yuan, X., and Jiao, Y.: Synergistic Effects of High-Resolution Factors for Improving Soil Moisture Simulations Over China, Water Resources Research, 59, e2023WR035513, 2023.
 - Jimma, T. B., Demissie, T., Diro, G. T., Ture, K., Terefe, T., and Solomon, D.: Spatiotemporal variability of soil moisture over Ethiopia and its teleconnections with remote and local drivers, Theoretical and Applied Climatology, 151, 1911–1929, 2023.
 - Jollife, I.: Principal component analysis 2 edition Springer, New York, 2002.

- Kang, H.-S. and Hong, S.-Y.: An assessment of the land surface parameters on the simulated regional climate circulations: The 1997 and 1998 east Asian summer monsoon cases, Journal of Geophysical Research: Atmospheres, 113, 2008.
 - Kato, H., Rodell, M., Beyrich, F., Cleugh, H., van GORSEL, E., Liu, H., and Meyers, T. P.: Sensitivity of land surface simulations to model physics, land characteristics, and forcings, at four CEOP sites, Journal of the Meteorological Society of Japan. Ser. II, 85, 187–204, 2007.
 - Koop, A. N., Hirmas, D. R., Billings, S. A., Li, L., Cueva, A., Zhang, X., Wen, H., Nemes, A., Souza, L. F., Ajami, H., et al.: Is macroporosity controlled by complexed clay and soil organic carbon?, Geoderma, 437, 116 565, 2023.
- 750 Korres, W., Koyama, C., Fiener, P., and Schneider, K.: Analysis of surface soil moisture patterns in agricultural landscapes using Empirical Orthogonal Functions, Hydrology and Earth System Sciences, 14, 751–764, 2010.
 - Koster, R. D., Suarez, M. J., Liu, P., Jambor, U., Berg, A., Kistler, M., Reichle, R., Rodell, M., and Famiglietti, J.: Realistic initialization of land surface states: Impacts on subseasonal forecast skill, Journal of hydrometeorology, 5, 1049–1063, 2004.
- Koster, R. D., Guo, Z., Yang, R., Dirmeyer, P. A., Mitchell, K., and Puma, M. J.: On the nature of soil moisture in land surface models,

 Journal of Climate, 22, 4322–4335, 2009.
 - Koukoula, M., Schwartz, C., Nikolopoulos, E., and Anagnostou, E.: Understanding the impact of soil moisture on precipitation under different climate and meteorological conditions: a numerical sensitivity study over the CONUS, Journal of Geophysical Research: Atmospheres, 126, e2021JD035 096, 2021.
- Kuss, A. J. M. and Gurdak, J. J.: Groundwater level response in US principal aquifers to ENSO, NAO, PDO, and AMO, Journal of Hydrology, 519, 1939–1952, 2014.
 - Lai, J. and Ren, L.: Estimation of effective hydraulic parameters in heterogeneous soils at field scale, Geoderma, 264, 28-41, 2016.
 - Lal, P., Singh, G., Das, N. N., Colliander, A., and Entekhabi, D.: Assessment of ERA5-land volumetric soil water layer product using in situ and SMAP soil moisture observations, IEEE Geoscience and Remote Sensing Letters, 19, 1–5, 2022.
- Lavers, D. A., Simmons, A., Vamborg, F., and Rodwell, M. J.: An evaluation of ERA5 precipitation for climate monitoring, Quarterly Journal of the Royal Meteorological Society, 148, 3152–3165, 2022.
 - Lawrence, D. M., Fisher, R. A., Koven, C. D., Oleson, K. W., Swenson, S. C., Bonan, G., Collier, N., Ghimire, B., van Kampenhout, L., Kennedy, D., et al.: The Community Land Model version 5: Description of new features, benchmarking, and impact of forcing uncertainty, Journal of Advances in Modeling Earth Systems, 11, 4245–4287, 2019.
- Lesinger, K. and Tian, D.: Trends, variability, and drivers of flash droughts in the contiguous United States, Water Resources Research, 58, e2022WR032 186, 2022.
 - Li, J., Duan, Q., Gong, W., Ye, A., Dai, Y., Miao, C., Di, Z., Tong, C., and Sun, Y.: Assessing parameter importance of the Common Land Model based on qualitative and quantitative sensitivity analysis, Hydrology and Earth System Sciences, 17, 3279–3293, 2013.
 - Linz, P. and Wang, R.: Exploring numerical methods: An introduction to scientific computing using MATLAB, Jones & Bartlett Learning, 2003.
- 775 Lorenz, E. N.: Empirical orthogonal functions and statistical weather prediction, vol. 1, Massachusetts Institute of Technology, Department of Meteorology Cambridge, 1956.
 - Martens, B., Miralles, D. G., Lievens, H., Van Der Schalie, R., De Jeu, R. A., Fernández-Prieto, D., Beck, H. E., Dorigo, W. A., and Verhoest, N. E.: GLEAM v3: Satellite-based land evaporation and root-zone soil moisture, Geoscientific Model Development, 10, 1903–1925, 2017.
- McDonough, K. R., Hutchinson, S. L., and Hutchinson, S.: Declining Soil Moisture Threatens Water Availability in the US Great Plains,
 Transactions of the ASABE, 63, 1147–1156, 2020.

- McNeill, S., Lilburne, L., Carrick, S., Webb, T., and Cuthill, T.: Pedotransfer functions for the soil water characteristics of New Zealand soils using S-map information, Geoderma, 326, 96–110, 2018.
- Melillo, J. M., Richmond, T., Yohe, G., et al.: Climate change impacts in the United States, Third national climate assessment, 52, 150–174, 2014.
- 785 Monahan, A. H., Fyfe, J. C., Ambaum, M. H., Stephenson, D. B., and North, G. R.: Empirical orthogonal functions: The medium is the message, Journal of Climate, 22, 6501–6514, 2009.
 - Montzka, C., Moradkhani, H., Weihermüller, L., Franssen, H.-J. H., Canty, M., and Vereecken, H.: Hydraulic parameter estimation by remotely-sensed top soil moisture observations with the particle filter, Journal of hydrology, 399, 410–421, 2011.
- Muñoz-Sabater, J., Dutra, E., Agustí-Panareda, A., Albergel, C., Arduini, G., Balsamo, G., Boussetta, S., Choulga, M., Harrigan, S., Hers-bach, H., et al.: ERA5-Land: A state-of-the-art global reanalysis dataset for land applications, Earth system science data, 13, 4349–4383, 2021.
 - Oleson, K. W., Lawrence, D. M., Bonan, G. B., et al.: Technical description of version 4.0 of the Community Land Model (CLM), NCAR Technical Note NCAR/TN-478+STR, 257, https://doi.org/10.5065/D6FB50WZ, 2010.
- Orth, R. and Seneviratne, S. I.: Analysis of soil moisture memory from observations in Europe, Journal of Geophysical Research: Atmospheres, 117, 2012.
 - Perry, M. A. and Niemann, J. D.: Analysis and estimation of soil moisture at the catchment scale using EOFs, Journal of Hydrology, 334, 388–404, 2007.
 - Qiao, L., Zuo, Z., and Xiao, D.: Evaluation of soil moisture in CMIP6 simulations, Journal of Climate, 35, 779-800, 2022.

800

- Reichle, R. H., Koster, R. D., Dong, J., and Berg, A. A.: Global soil moisture from satellite observations, land surface models, and ground data: Implications for data assimilation, Journal of Hydrometeorology, 5, 430–442, 2004.
- Reichle, R. H., Draper, C. S., Liu, Q., Girotto, M., Mahanama, S. P., Koster, R. D., and De Lannoy, G. J.: Assessment of MERRA-2 land surface hydrology estimates, Journal of Climate, 30, 2937–2960, 2017.
- Sanchez-Murillo, R., González-Hita, L., Mejía-González, M. A., Carteño-Martinez, B., Aparicio-González, J. C., Mañón-Flores, D., Ortega, L., Stojanovic, M., Nieto, R., and Gimeno, L.: Tracing isotope precipitation patterns across Mexico, PLOS Water, 2, e0000 136, 2023.
- Schaap, M. G., Leij, F. J., and Van Genuchten, M. T.: Neural network analysis for hierarchical prediction of soil hydraulic properties, Soil Science Society of America Journal, 62, 847–855, 1998.
 - Schaap, M. G., Leij, F. J., and Van Genuchten, M. T.: Rosetta: A computer program for estimating soil hydraulic parameters with hierarchical pedotransfer functions, Journal of hydrology, 251, 163–176, 2001.
- Silwimba, K.: kachingasilwimba/spmip-eof-analysis: CLM5 SPMIP EOF Analysis Toolkit, https://doi.org/10.5281/zenodo.14888812, 2025a.
 - Silwimba, K.: Soil Moisture Data Subset from the Community Land Model Version 5 (CLM5) for the Soil Parameter Model Intercomparison Project (SP-MIP) over the Continental United States (CONUS), 1980-2010, https://doi.org/10.5281/zenodo.15078448, 2025b.
 - Sullivan, P. L., Billings, S. A., Hirmas, D., Li, L., Zhang, X., Ziegler, S., Murenbeeld, K., Ajami, H., Guthrie, A., Singha, K., et al.: Embracing the dynamic nature of soil structure: A paradigm illuminating the role of life in critical zones of the Anthropocene, Earth-Science Reviews, 225, 103 873, 2022.
 - Tafasca, S., Ducharne, A., and Valentin, C.: Weak sensitivity of the terrestrial water budget to global soil texture maps in the ORCHIDEE land surface model, Hydrology and Earth System Sciences, 24, 3753–3774, 2020.

- Tang, L. I. and McColl, K. A.: An Observational, Irrigation-Sensitive Agricultural Drought Record from Weather Data, Journal of Hydrometeorology, 24, 2091–2103, 2023.
- Taylor, K. E.: Summarizing multiple aspects of model performance in a single diagram, Journal of geophysical research: atmospheres, 106, 7183–7192, 2001.
 - Thornton, E.: Technical Description of version 4.0 of the Community Land Model (CLM), NCAR, Climate and Global, 2010.
 - Tobin, K. J., Crow, W. T., Dong, J., and Bennett, M. E.: Validation of a new root-zone soil moisture product: Soil MERGE, IEEE Journal of Selected Topics in Applied Earth Observations and Remote Sensing, 12, 3351–3365, 2019.
- Tuttle, S. and Salvucci, G.: Empirical evidence of contrasting soil moisture–precipitation feedbacks across the United States, Science, 352, 825–828, 2016.
 - Van den Hurk, B., Kim, H., Krinner, G., Seneviratne, S. I., Derksen, C., Oki, T., Douville, H., Colin, J., Ducharne, A., Cheruy, F., et al.: LS3MIP (v1. 0) contribution to CMIP6: the Land Surface, Snow and Soil moisture Model Intercomparison Project–aims, setup and expected outcome, Geoscientific Model Development, 9, 2809–2832, 2016.
- Van Looy, K., Bouma, J., Herbst, M., Koestel, J., Minasny, B., Mishra, U., Montzka, C., Nemes, A., Pachepsky, Y. A., Padarian, J., et al.:

 Pedotransfer functions in Earth system science: Challenges and perspectives, Reviews of Geophysics, 55, 1199–1256, 2017.
 - Vereecken, H., Weynants, M., Javaux, M., Pachepsky, Y., Schaap, M., and Genuchten, M. T. v.: Using pedotransfer functions to estimate the van Genuchten–Mualem soil hydraulic properties: A review, Vadose Zone Journal, 9, 795–820, 2010.
- Weber, T. K., Finkel, M., da Conceição Gonçalves, M., Vereecken, H., and Diamantopoulos, E.: Pedotransfer function for the Brunswick soil hydraulic property model and comparison to the van Genuchten-Mualem model, Water resources research, 56, e2019WR026 820, 2020.
 - Welty, J. and Zeng, X.: Does soil moisture affect warm season precipitation over the southern Great Plains?, Geophysical Research Letters, 45, 7866–7873, 2018.
 - Wipfler, E., Metselaar, K., Van Dam, J., Feddes, R., Van Meijgaard, E., Van Ulft, L., van den Hurk, B., Zwart, S. J., and Bastiaanssen, W. G.: Seasonal evaluation of the land surface scheme HTESSEL against remote sensing derived energy fluxes of the Transdanubian region in Hungary, Hydrology and earth system sciences, 15, 1257–1271, 2011.

840

- Wu, Z., Feng, H., He, H., Zhou, J., and Zhang, Y.: Evaluation of soil moisture climatology and anomaly components derived from ERA5-land and GLDAS-2.1 in China, Water Resources Management, 35, 629–643, 2021.
- Ye, S., Liu, L., Li, J., Pan, H., Li, W., and Ran, Q.: From rainfall to runoff: The role of soil moisture in a mountainous catchment, Journal of Hydrology, 625, 130 060, 2023.
- Yuan, S. and Quiring, S. M.: Evaluation of soil moisture in CMIP5 simulations over the contiguous United States using in situ and satellite observations, Hydrology and Earth System Sciences, 21, 2203–2218, 2017.
 - Zeng, J., Yuan, X., Ji, P., and Shi, C.: Effects of meteorological forcings and land surface model on soil moisture simulation over China, Journal of Hydrology, 603, 126 978, 2021.
- Zhang, L., Kim, T., Yang, T., Hong, Y., and Zhu, Q.: Evaluation of Subseasonal-to-Seasonal (S2S) precipitation forecast from the North

 American Multi-Model ensemble phase II (NMME-2) over the contiguous US, Journal of Hydrology, 603, 127 058, 2021.
 - Zhang, L., Yang, Y., Liu, Y., and Yue, X.: Evaluation of Long Time-Series Soil Moisture Products Using Extended Triple Collocation and In Situ Measurements in China, Atmosphere, 14, 1351, 2023.
 - Zhao, F., Veldkamp, T. I., Frieler, K., Schewe, J., Ostberg, S., Willner, S., Schauberger, B., Gosling, S. N., Schmied, H. M., Portmann, F. T., et al.: The critical role of the routing scheme in simulating peak river discharge in global hydrological models, Environmental Research Letters, 12, 075 003, 2017.